Transport Studies of Chondroitin Sulfate Disaccharide Through Articular Cartilage

by

Julianne Jiang Zhu

Submitted to the Department of Electrical Engineering and Computer Science in Partial Fulfillment of the Requirements for the Degree of

Master of Engineering in Electrical Engineering and Computer Science

at the

MASSACHUSETTS INSTITUTE OF TECHNOLOGY

May 1997

Author .....
Department of Electrical Engineering and Computer Science
Date Submitted

Certified by .....
Alan J. Grodzinsky
Thesis Supervisor

Accepted by .....
Arthur C. Smith
Chairman, Department Committee on Graduate Theses

Transport Studies of Chondroitin Sulfate Disaccharide Through Articular Cartilage

by

Julianne Jiang Zhu

Submitted to the
Department of Electrical Engineering and Computer Science

May 1997

In partial fulfillment of the requirements for the degree of
Master of Engineering in Electrical Engineering and Computer Science

Abstract

The load bearing ability of articular cartilage is dependent on the integrity of the extracellular matrix. The maintenance and repair of the tissue matrix by chondrocyte biosynthetic activities rely on the movement of solutes through the matrix. To understand the factors which affect solute transport through the articular cartilage, study of the transport properties of disaccharides through adult steer articular cartilage explants was conducted. Cartilage disks were harvested from the femoropatellar groove of adult steer. The tissue disks were mounted in a two compartment transport chamber. Radiolabelled disaccharides were added to the upstream compartment, and changes in radioactivity were monitored in the downstream compartment. Disaccharide diffusion coefficient of $4.49 \pm 1.13 \times 10^{-6}$ cm^2/sec (mean$\pm$SD) was calculated using the measured steady state diffusive flux and the measured partition coefficient of 1.12 ± 0.52 (mean$\pm$SD). Electric current densities were applied across the articular cartilage disks to induce electroosmotic fluid flow within the tissue matrix. Application of negative current densities elevated the disaccharide flux over the steady state diffusive flux by a factor of 2.36 ± 1.15 (mean$\pm$SD), and application of positive current densities depressed the disaccharide flux under the steady state diffusive flux by a factor of 0.055 ± 0.94 (mean$\pm$SD). Electromigration played the dominant role in solute flux during current applications.

Thesis Supervisor: Alan J. Grodzinsky
Title: Professor of Electrical, Mechanical, and Bioengineering, M.I.T

Acknowledgments

My heartfelt appreciation to:

Alan Grodzinsky for your endless patience, encouragement, motivation, and inspiration. It has been an honor and a pleasure to have been a part of the Continuum Electromechanics Lab.

Minerva Garcia, my mentor. Thank you for you guidance, advise, kindness, and friendship. I could not have done this work without you.

Eliot Frank for debugging all my mysterious problems with the transport equipments. Your vast knowledge on science and electronics amazes me.

Dr. Anna Plaas for providing me with the radiolabelled disaccharides.

Michelle Jen for laying down the ground work for my study, Nirav Bhakta for helping me with the transport equipments, Jane Murray for introducing me to the laboratory basics, Ann Black for generously providing me with solutions for my experiments, and Linda Gragman for your spirit and humor.

Steve for driving me to the slaughter house, Paula for being a wonderful TA in 6.561, Marc for your eagerness to help with everything, Adil for helping me with FrameMaker, Larry for your friendly inquires about my work, and everyone else in the Continuum Electromechanics Lab.

Sara for being a wonderful friend since high school, Winnie, Erin, Rachel, and Maryann for five laughable years at MIT, Nitin for our thought provoking tea times, Jesse for showing me how to be spontaneous, and Bill for your unconditional friendship.

Sang for your coaching and friendship, Caroline, Sue-ann, Betty, Betty, Arline, Tomoko, Nara, Sharron, Maurice, Edwin, Steve, John, and John for all the fun times playing volleyball.

Kai Lee for your understanding, consideration, generosity, and sensitivity. You have made 1997 a unforgettable year for me.

My parents for everything you have done for me in life.

Table of Contents

List of Figures

List of Tables

List of Symbols

CPM	counts per minute
CS	chondroitin sulfate
ECM	extracellular matrix
EDTA	ethylenedinitrilo tetraacetic acid
FCD	fixed charge density
GAG	glycosaminoglycan
HEPES	N-2-hydroxyethylpiperazine-N'-2-ethanesulfonic acid
KS	keratan sulfate
PBS	phosphate buffered saline
PA	polyacrylamide
PG	proteoglycan
PMSF	phenylmethylsulfonyl fluoride

$\underline{A}$	cross-sectional tissue area for transport
$\overline{c}_{di}$	intratissue concentration of disaccharide
$c_{di,u}$	disaccharide concentration in the upstream bath
$\underline{c}_i$	concentration of solute i in the external solution
$\overline{c}_i$	intratissue concentration of solute i
$\underline{c}_x$	concentration of cation x in the external solution
$\overline{c}_x$	intratissue concentration of cation x
$\underline{c}_y$	concentration of anion y in the external solution
$\overline{c}_y$	intratissue concentration of anion y
CPM_d	counts per minute of the downstream bath
ΔCPM_d	change in counts per minute of the downstream bath
$\Delta CPM_{d,cal}$	counts per minute of the medium normalized to the medium volume
CPM_m	counts per minute of the medium normalized to the medium volume
CPM_t	counts per minute of the tissue normalized to the water content of the tissue
$\overline{D}_{di}$	disaccharide diffusion coefficient
D_i	diffusion coefficient of solute i in water
$\overline{D}_i$	intratissue diffusion coefficient of solute i
E	electric field
F	Faraday constant = 9.6487×10^4 coul/mol
J	one dimensional electrical current density
$\overline{J}$	electrical current density
K	partition coefficient
k_{11}	short circuit Darcy hydraulic permeability
k_{12}, k_{21}	electrokinetic coupling coefficients
k_{22}	electrical conductivity
K_{di}	disaccharide partition coefficient
P	fluid pressure
Δt	change in time
U	intratissue fluid velocity
$\overline{U}$	relative fluid velocity
V	electrical potential

V_d	downstream bath volume
$V_{u,cal}$	upstream bath calibration volume
z_i	valence of solute i
δ	tissue thickness
ϕ	tissue thickness
Γ_{di}	disaccharide flux
Γ_i	flux of solute i
$\underline{\mu}_i$	valence of solute i
$\overline{\rho}_m$	fixed charge density of the tissue

Chapter I

Introduction

1.1 Articular Cartilage

Articular cartilage provides the low-friction wear-resistant bearing surface that distributes and transmits loads to the underlying bone surface in the synovial joint. The ability of articular cartilage to withstand compressive, tensile, and shear forces is dependent on the composition and structural integrity of the extracellular matrix (ECM). A schematic of the articular cartilage is shown in Figure 1.1. Constituents of articular cartilage are: structural macromolecules, abundant tissue fluid, and chondrocytes. The maintenance and repair of functional ECM by chondrocytes in the articular cartilage require the coordinated synthesis, assembly, and turnover of ECM macromolecules. As the articular cartilage matrix assembly proceeds, newly synthesized macromolecules secreted by chondrocytes are transported through the matrix and become immobilized at their ultimate destination; macromolecule fragments resulting from matrix degradation are transported out of the matrix as waste products. Chondrocyte biosynthetic activities rely on the movement of solutes through the matrix to and from the synovial fluid in the joint. Regulation of the metabolic process involves a combination of electromechanical and physicochemical mechanisms. Variations in environmental conditions and applications of various stimuli to the articular cartilage can lead to elevation or depression of the matrix metabolism and turnover [3,5,6,13,14].

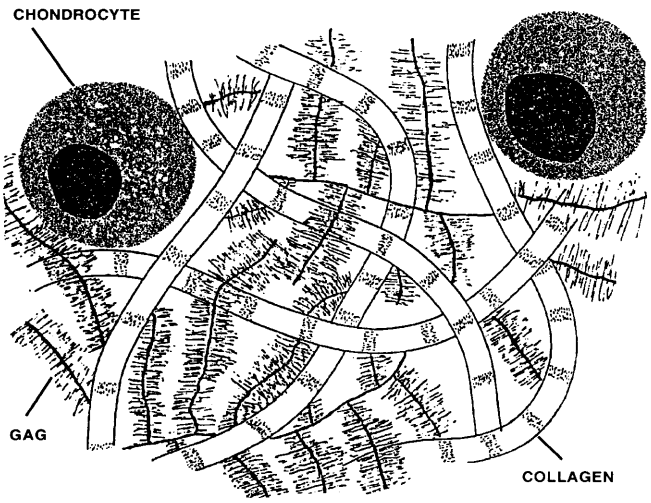

Figure 1.1: Schematic of the articular cartilage adapted from [2].

1.2 Articular Cartilage Composition and Structure

1.2.1 Structural Macromolecules

Structural macromolecules, consisting of collagens, proteoglycans (PG), and noncollagenous proteins, contribute 20% to 40% of the articular cartilage wet weight. Collagens contribute 50% of the tissue's dry weight, proteoglycans contribute 30% to 35%, and noncollagenous proteins contribute 15% to 20% [12]. Collagen fibrils provide the articular cartilage with tensile and shear resistance; proteoglycans, containing anionic charge groups at physiologic conditions, account for the significant compressive strength of the articular cartilage; and noncollagenous proteins help to organize and maintain the macromolecular structure of the articular cartilage EMC and the relationship between chondrocytes and the tissue matrix.

Collagen The primary structure protein of the body is collagen. The collagen molecule consists of three 300nm long and 1.5nm in diameter helical amino acid chains. The amino acid within each chain is arranged in a helical pattern with 3.27 residues per turn [11]. Collagen, with its chain-like molecular structure and extensive cross-linking, forms the cross-banded collagen fibril network in the EMC. Different polypeptide chain amino acid sequences classify collagens into different types of molecules. The principle collagen of the articular cartilage is type II collagen, accounting for 90% to 95% of the total articular cartilage collagen. Type II collagen establishes an ordered relationship with PGs, thus creating and maintaining the highly hydrated matrix in the articular cartilage. Intermolecular cross-linking of type II collage fibrils determines the tensile strength of the collagen network and of the tissue. Type IX and XI collagens account for 3% of the collagen in the articular cartilage. Type IX collagen contains collagenous and noncollagenous domains. The molecular structure of type IX collagen provides the potential interface between the collagenous framework in the tissue and the PG substance, and provides reinforcement and stabilization of the type II collagen fibril network. Type XI collagen provides the formation of heterotypic fibrils with type II collagen molecules. Type VI and X collagens account for 1% of the articular cartilage collagen. Type VI collagen, with its distinct cross-linking behavior, plays a role in cell attachment. Type X collagen is associated with the hypertrophic zone in the growth plate articular cartilage [1].

Proteoglycan Proteoglycan forms the major macromolecule of cartilage ground substance. PG macromolecules exist in multiple forms: as nonaggregating PGs, as aggregating PG monomers, and as aggregates containing multiple PG monomers. The aggregating PG monomer, shown in Figure 1.2, consists of protein core filament with multiple covalently bound oligosaccharides

and chondroitin and keratan sulfate chains. The protein core has three globular domains: two at the N-terminal region, G1 and G2, and one at the C-terminal region, G3 [7]. Three different regions are located along the protein core filament: the hyaluronate binding region, the keratan sulfate-rich region, and the chondroitin sulfate-rich region. The hyaluronate binding region, at the G1 domain, has the ability to associate reversibly with the hyaluronic acid and the link protein. The keratan sulfate-rich region, near the G2 domain, binds 60% of the total keratan sulfate found in the molecule. The chondroitin sulfate-rich region, between the keratan sulfate-rich region and the G3 domain, binds 90% of the total chondroitin sulfate [1]. The keratan and the chondroitin sulfate-rich regions, between the G1 and the G2 domains, are the glycosaminoglycan-rich regions of the PG unit. Glycosaminoglycans (GAGs) form from chains of negatively charged disaccharides, including chondroitin-4-sulfates, chondroitin-6-sulfates, and keratan sulfate. A schematic of the chondroitin-6-sulfate disaccharide unit with ionized carboxyl and sulfate groups is shown in Figure 1.3. Adjacent GAG chains, containing large number of negative charges, repel each other in the extracellular matrix, and maintain the molecule in an expanded form. GAGs, chondroitin sulfates and keratan sulfates contribute 95% of the molecule and proteins contribute 5%. In the EMC, aggregating proteoglycan monomers associate noncovalently with hyaluronic acid filaments and link proteins to form aggregates. Hyaluronic acids form the backbone of the aggregate. Link proteins stabilize the association between monomers and hyaluronic acid filaments and play a role in directing the assembly of aggregates [11].

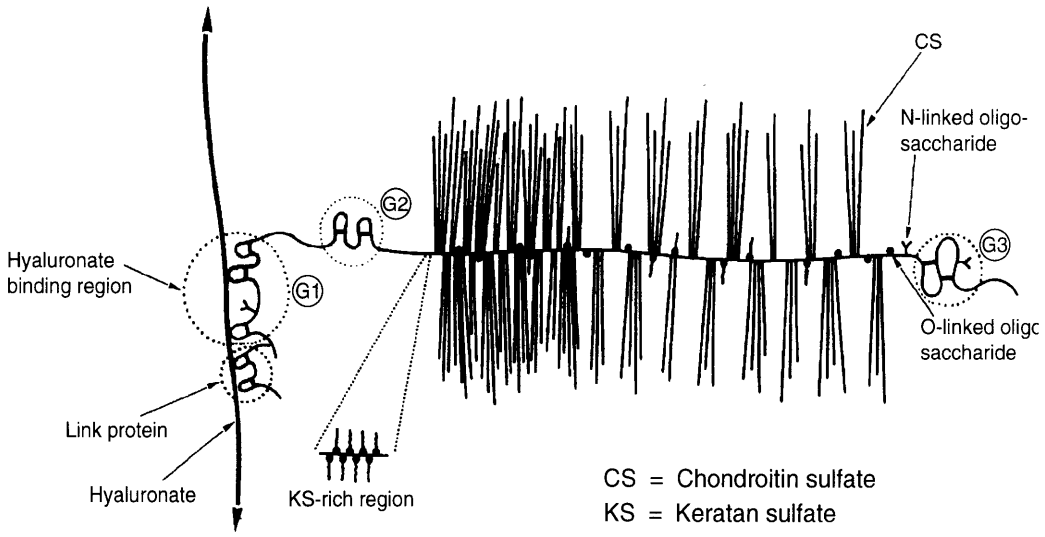

Figure 1.2: Schematic of the proteoglycan monomer adapted from [7].

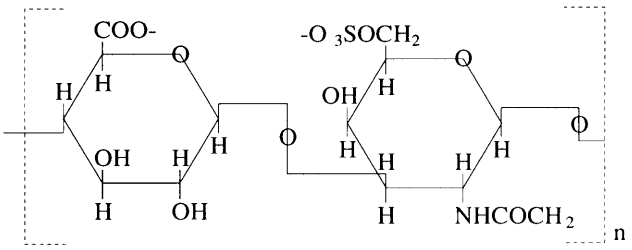

Figure 1.3: Schematic of the chondroitin-6-sulfate disaccharide unit.

The PG is responsible for the most important characteristics of the articular cartilage. The ability of PG to interact with tissue fluid gives articular cartilage the stiffness for compression and resilience and contributes to the durability of the tissue. The flexible, hydrophilic negatively charged GAG chain gives the EMC a high swelling pressure. The PG aggregate network, interacting with the collagen fibril network, ensures a low hydraulic permeability of articular cartilage. Combining with the high water content of the articular cartilage, PG contributes to the tissue's load-bearing property and low coefficient of friction. The selective behavior of the matrix to the penetration of solutes is dependent on the concentration of negatively charged groups and the density of the PG network. Variations of the PG content and of electromechanical and physicochemical signals in the articular cartilage lead to changes in the behavior of the tissue.

Noncollagenous Proteins The link protein, the chondronectin, and the anchorin CII are noncollagenous proteins in the articular cartilage. Chondronectin and anchorin CII both mediate adhesion of chondrocytes to the molecular type II collagen framework of the ECM. The chondronectin is located in the matrix and only binds to the collagen in the presence of chondroitin sulfates. The anchorin CII is located in the pericellular space of the articular cartilage matrix directly adjacent to chondrocytes, but not in the intercellular matrix [1].

1.2.2 Tissue Fluid

Tissue fluid, consisting of water with dissolved gases, small proteins, and metabolites, is the major constituent of the articular cartilage as it contributes 60% to 80% of the wet weight of the tissue [1]. The high water content of the tissue provides the matrix with a medium for solute transport. The fluid content of the tissue is determined by the balance between the swelling pressure of the PG network and the tension in the collagen network. While the collagen fibril network prevents full expansion of PGs and thus diminishes water inflow, the GAG component regulates the intrafibillar water content with the osmotic pressure exerted over the surface of collagen fibrils. Since the

tissue fluid is not contained within the cellular membrane, its volume, concentration, organization and behavior depend on the balanced interactions between structural matrix molecules. Higher water content is observed in the fibrillated articular cartilage, and lower water content in the articular cartilage is observed with aging. In the fibrillated tissue, the collagen network is damaged, thus decreases the ability to restrain the PG's swelling pressure and increases the water content of the tissue. The trend in a uniform decrease in the water content with aging is due to the greater degree of cross-linking in the collagen fibril network, thus lowers the extensibility of the EMC and decreases the water content of the cartilage [10].

1.2.3 Chondrocytes

Chondrocytes contribute 10% of the articular cartilage by volume. Material properties of the articular cartilage depend on the ECM, and the existence and maintenance of the matrix depend on chondrocytes. Chondrocytes in the articular cartilage maintain the mechanically functional ECM by regulating synthesis and degradation of matrix constituents. Chondrocytes have organelles responsible for cell matrix synthesis, and additionally contain intracytoplasmic filaments, glycogens, and cilia to regulate matrix turnover [1]. Chondrocyte synthetic function alters changes in matrix composition and changes in tension on the cell membrane. Chondrocytes regulate and repair ECM by secreting and interacting with factors mediating the matrix assembly. Cells proliferate rapidly during articular cartilage formation and synthesize large volumes of the matrix. The process slows down and the cell density decreases with maturation of the tissue. The decrease in cell density and cell synthetic function limits the ability of chondrocytes to restore the damaged cartilage matrix.

1.3 Previous Articular Cartilage Transport Research

1.3.1 Partition

The equilibrium concentration of a solute in the articular cartilage depends on three factors: the concentration of the solute in the synovial fluid; the consumption or production of the solute by chondrocytes in the tissue; and the distribution of the solute between the synovial fluid and the articular cartilage [10]. The distribution of the solute between the articular cartilage and the external solution is quantitatively described by its partition coefficient. The partition coefficient, K, is defined as the ratio of the concentration of the solute in the tissue, $\bar{c}_i$, to the concentration of the

solute in the external solution, c_i. Partition coefficient is the measurement of the affinity of the solute towards the tissue. A partition coefficient of 1.0 indicates that the solute distributes itself in the tissue the same as in the free external solution, a coefficient less than one indicates an exclusion of the solute by the tissue, and a coefficient greater than one indicates an affinity for the solute by the tissue. Factors that affect the partition coefficient of the solute in the articular cartilage are: the solute's size and shape, the solute's charge, and the fixed charge density (FCD) of the EMC. Table 1.1 lists Maroudas *et. al.*'s [10] partition coefficients for various solutes between the articular cartilage and external solutions at FCD of 0.08 mEq g^{-1} (34 mg/ml) and FCD of 0.16 mEq g^{-1} (68.3 mg/ml). Table 1.2 lists Jen's [8] partition coefficients for GAG chain and aggrecan monomer between the articular cartilage and external solutions at FCD of 20mg/ml, FCD of 30mg/ml, and FCD of 40mg/ml.

Solute	Molecular Weight (Da)	FCD=34 mg/ml	FCD=68 mg/ml
Small neutral solutes			
Tritiated water	18	1.0	1.0
Urea, proline	60	1.0	1.0
Glucose	180	1.0	0.9
Sucrose	380	1.0	0.9
Small cations			
Na^+	23	1.5	2.2
Ca^{2+}	40	3	9
Small anions			
Cl^-	35.5	0.75	0.53
SO_4^{2-}	96	0.6	0.4
Large solutes			
Serum albumin	69,000	0.01	0.001
IgG	160,000	0.01	0.001

Table 1.1: Partition coefficients of solutes between the articular cartilage and external solutions adapted from [10].

Solutes	FCD=20 mg/ml	FCD=30 mg/ml	FCD=40 mg/ml
GAG chain	0.1-0.6	0.1-0.4	0.12-0.32
Aggrecan monomer	0.09-0.15	0.08-0.11	0.05-0.1

Table 1.2: Partition coefficients of GAG chains and aggrecan monomers between the articular cartilage and external solutions.

The method for partition coefficient measurements used by Jen and Maroudas *et al* is [8,9]: equilibration of the articular cartilage in the solution with the radioactively labelled solute in a known amount of the unlabeled solute; then the digestion of the tissue, or the desorbtion of the tracer by subsequent equilibration of the tissue with a series of unlabeled solutions. The partition coefficient of the solute is calculated from the measured amount of tracer in the articular cartilage and amount of the radiolabeled solute in the initial equilibrating solution.

Partition coefficients of small neutral solutes between the articular cartilage and external solutions are close to unity and independent of the GAG content, thus implying that small solutes distribute equally between all of the cartilage water, either the water is inter- or intrafibillar water. Small cations and anions have partition coefficients greater than and less than one respectively. For cations, partition coefficients increase with the FCD; and for anions, coefficients decrease with the FCD. The variation in partition coefficients of charged solutes with the FCD indicates that negatively charged GAGs in the tissue's EMC interact with charged solutes, and are responsible for the concentrations of charged solutes in the articular cartilage. Partition coefficients of large globular solutes decrease with increasing molecular weight and with increasing FCD. Partition coefficients of large globular solutes are more sensitive to variations in FCD than to variations in solute molecular weight. For solutes larger than serum albumin, partition coefficients no longer decrease with increasing sizes, thus indicating that the transport of these larger solutes occurs mainly through the small population of pores much larger than the 90A average pore [10].

1.3.2 Diffusion

The rate of diffusion of a solute between the external solution and the articular cartilage is governed by three factors: the resistance of a stagnant liquid film at the articular cartilage/fluid interface; the partition coefficient of the solute between the tissue and the external solution; and the effective diffusion coefficient of the solute in articular cartilage [9]. Diffusion coefficients charac-

terize mobilities of solutes. Table 1.3 lists Maroudas *et. al.*'s [10] diffusion coefficients for various solutes in the articular cartilage, $\overline{D}_i$, and the ratios of diffusion coefficient of the solutes to that in water, $\overline{D}_i/D_i$. Table 1.4 lists Jen's [8] diffusion coefficients for GAG chain and aggrecan monomer in the articular cartilage.

Solutes	Molecular Weight (Da)	Temperature	$\overline{D}_i$ ($cm^2/s \times 10^{-6}$)	$\overline{D}_i/D_i$
Small neutral solutes				
Tritiated water	18	8°C	6-7	0.4-0.45
		37°C	12-14	0.4-0.45
Urea, proline	60	25°C	6.0	0.4-0.45
Glucose	180	25°C	2.4-2.7	0.4-0.45
Sucrose	380	25°C	1.9-2.1	0.4-0.45
Small cations				
Na^+	23	25°C	4.8-5.5	0.4
Ca^{2+}	40	25°C	1.5	0.25
Small anions				
Cl^-	35.5	25°C	7.5-8.5	0.4-0.45
SO_4^{2-}	96	37°C	2.8-3.5	0.4-0.45
Large solutes				
Serum albumin	69,000	8°C	0.1	0.25
		25°C	0.16	
IgG	160,000	8°C	0.5	0.2

Table 1.3: Diffusion coefficients of solutes in the articular cartilage adapted from [10].

Solutes	Temperature	$\overline{D}_i$ ($cm^2/s \times 10^{-8}$)
GAG chain	20°C	0.496-1.23
Aggrecan monomer	20°C	8.58-10.6

Table 1.4: Diffusion coefficients of GAG chains and aggrecan monomers in the articular cartilage.

Two methods for diffusion coefficient measurements used by Jen [8] and Maroudas *et al* [9] are: the permeability method and the sorption-desorption method. The permeability method uses the articular cartilage as a membrane between two separate chamber of solutions: one solution contains the radiolabelled solute of interest, and the other solution contains none. The flux of a given solute across the membrane is measured by monitoring the radiolabelled solute in the originally non-radiolabelled solution. The diffusion coefficient of the solute is then calculated using the flux measurement and the partition coefficient [4]. The sorption-desorption method equilibrates the articular cartilage in solution with the radiolabelled solute. The tissue is desorbed in a series of solutions without the radiolabelled solute until no further tracer is left in the desorbate solution. Diffusion coefficient is then predicted with the total amount of radiolabelled solute desorbed as a function of time [4].

The ratios of diffusion coefficients of small neutral solutes in the articular cartilage and in free solution are between 0.4 and 0.45. The reduction in diffusion coefficients in the articular cartilage as compared with the free solution is due to the reduction in the effective area available to diffusing molecules, and the increase in the diffusion path obstruction provided by solid constituents of the matrix. As observed previously in small neutral solutes, small cations and anions in the articular cartilage have diffusion coefficients equal to 25%-45% of diffusion coefficient values in the free solution. Due to the existence of electrostatic interactions between ions and negatively charged GAGs: cations have lower $\overline{D}_i/D_i$s and anions have higher $\overline{D}_i/D_i$s than small neutral solutes. The ratio $\overline{D}_i/D_i$ of Ca^{2+} is 25%, 10%-20% lower than the $\overline{D}/D$ of Cl^-. Interactions between small charged solutes and negatively charged GAGs, however, are relatively weak. Thus, for solute that is small in comparison with the cross-sectional area of pores in the EMC, the movement of the solute is governed mainly by free diffusion, and the ratio of the diffusion coefficient in the tissue to that in the water being dependent mainly on the water content of the tissue and the density of the EMC [9]. The diffusion coefficients of large globular solutes, whose dimensions are significant in relation to the tissue pore size, depend not only on frictions between solutes and the solvent but also on frictions between solute molecules and solid elements in the matrix. Maroudas *et. al.* [10] observed that diffusion through the articular cartilage diminishes with increasing size of solutes. Once the interactions between the solute and the matrix are significant, however, more than just the molecular size of the solute effects its diffusion. The shape of the solute, the FCD of the tissue and the heterogeneous matrix pore structure effect the transports of large solutes through the

articular cartilage more than for small solutes. Thus, for large solutes, mobilities are governed mainly by partition coefficients rather than diffusivities.

1.3.3 Electroosmosis

Electroosmosis is the fluid flow occurring through a charged solid medium in contact with an electrolyte solution in response to an applied electric field. Application of an electric field across the charged membrane causes migration of predominate mobile counterions within the membrane. The momentum of counterions is then transferred to the surrounding fluid due to viscous interactions. The magnitude and direction of the induced electroosmotic fluid flow in the articular cartilage depend on the value of the applied electric field and the fixed charge density of the tissue. Figure 1.4 shows Garcia's [2] measurements of electroosmotic fluid flow across the articular cartilage for applied current density, J, of -10, 0, 10, 20, and 30 mA/cm^2.

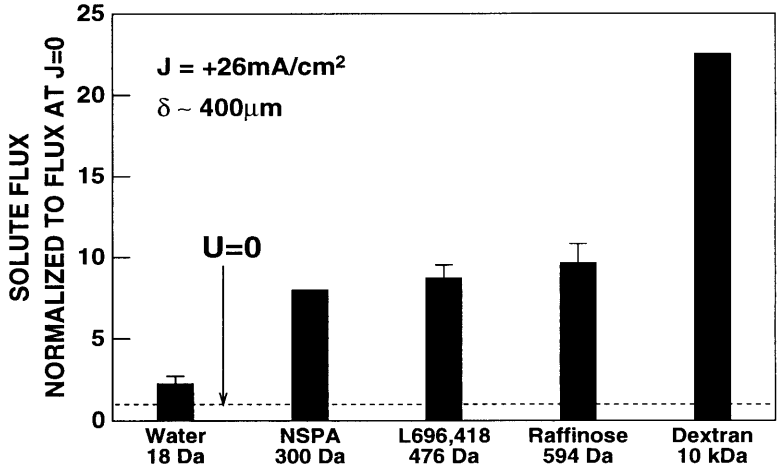

Figure 1.4: Electroosmotic fluid flow across the articular cartilage adapted from [2].

The method for electroosmosis measurements used by Garcia [2] uses the articular cartilage as the partition between two separate chamber of deaerated saline solutions. One of the chambers is air-tight and connected by capillary tubing to a beaker positioned on a microbalance. Various steady current densities are applied for 20 minutes at each level. The net flux flow across the membrane is then measured by monitoring the weight of the beaker. The increase in weight versus time is normalized to the total exposed tissue area to calculate the intratissue fluid velocity at each current density.

The induced fluid flow through the articular cartilage, containing negatively fixed charge density, is in the same direction of the applied current density. The electroosmotic fluid velocity within

the articular cartilage is found to increase linearly with applied current density. A change in polarity of the applied current reverses the direction of the measured fluid flow, however, does not change the magnitude of the fluid velocity.

1.3.4 Convection

Convective flux reflects the motion of the medium in solute transport. The rate of fluid convection in the articular cartilage is governed by the intratissue concentration of the solute and the intratissue fluid velocity induced by the applied electric field. For solute transport in the negatively charged membrane, the direction of convective electroosmotic fluid flow is in the direction of the applied electric field. For solute transport in the positively charged membrane, the direction of convective electroosmotic fluid flow is in the opposite direction of the applied electric field. Figure 1.5 shows Garcia's [2] measurements of electroosmotic fluid convections of neutral solutes through the articular cartilage with applied current density of +26 mA/cm^2. The solute flux in the presence of current is normalized to the solute flux in the absence of current.

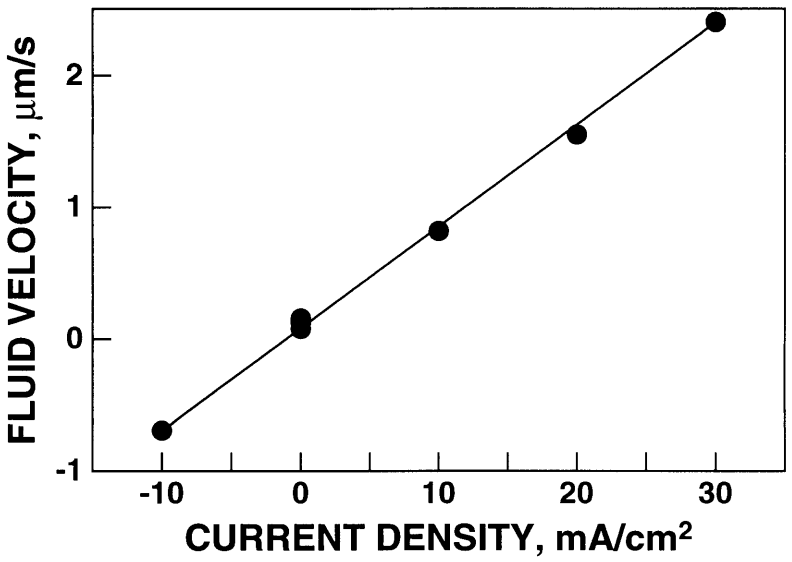

Figure 1.5: Fluid convections of neutral solutes through the articular cartilage adapted from [2].

The method for fluid convection measurements used by Garcia [2] uses the articular cartilage as the partition between two separate chamber of solutions: one solution contains the radiolabelled neutral solute of interest, and the other solution contains none. After steady state diffusion of the solute is obtained, current density of + 26 mA/cm^2 is applied across the membrane to induce intratissue fluid velocity. The net fluid flow of the neutral solute across the membrane is then mea-

sured by monitoring the radiolabelled solute in the originally non-radiolabelled solution. For the neutral solute, electrical migration has no contribution to solute transport, thus any change in the solute flux from the steady state diffusion is caused by convection. The net flux flow is then a direct measure of the relative contributions of convection and diffusion to the total solute flux.

The ratios of solute flux in the presence of positive current to the flux in the absence of current increase with increasing solute size. Solute diffusivity within the articular cartilage decreases as solute size increases, and ratio of fluid convection to diffusion becomes larger. Thus, the relative contribution of fluid convection is more significant for larger solutes than smaller solutes.

1.3.5 Electrical Migration

Electrical migration flux reflects the motion of ions in solute transport. The value of electrically induced migration depends on electrophoretic flow of the solute. Electrophoresis is the movement of solute through electrolyte solution in response to an applied electric field: cations migrate towards the cathode and anions migrate towards the anode. The direction of electrophoretic flow is determined by the charge of the solute and the direction of the applied electric field. For negative solute transport in the articular cartilage, the direction of electrical migration opposes the convective electroosmotic fluid flow. For positive solute transport in the articular cartilage, the direction of electrical migration enhances the convective electroosmotic fluid flow. Table 1.5 lists Jen's [8] measurements of net fluxes of the negatively charged GAG chain and the aggrecan monomer through the articular cartilage with applied current densities of -26 and +26 mA/cm^2.

Solutes	Flux (CPM/minute)		
Current density	0 mA/cm^2	-26 mA/cm^2	+26 mA/cm^2
GAG chain	0.005	0.3	-0.09
Aggrecan monomer	0.06	1.2	-0.4

Table 1.5: Net fluxes of negatively charged solutes through the articular cartilage.

The method for electrical migration measurements used by Jen [8] uses the articular cartilage as the partition between two separate chamber of solutions: one solution contains the radiolabelled charged solute of interest, and the other solution contains none. After steady state diffusion of the solute is obtained, current densities of -26 and +26 mA/cm^2 were applied separately across the

membrane. The net flux flow of the solute across the membrane is then measured by monitoring the radiolabelled solute in the originally non-radiolabelled solution.

The net fluxes of the GAG chain and the aggrecan monomer increase in the direction of diffusive flow with an applied negative current density of -26 mA/cm^2, and the net fluxes increase in the opposite direction of diffusive flow with an applied positive current density of +26 mA/cm^2. The increases in the magnitude of net fluxes of the GAG chain and the aggrecan monomer are higher for the application of negative current densities than the application of positive current densities. For the negative current density application across the articular cartilage, diffusive and electrical migration fluxes are in the opposite direction of the applied current, while convective flux is in the same direction of the applied current. For the positive current density application, diffusive and convective fluxes both are in the same direction of the applied current, while electrical migration flux is in the opposite direction of the applied current. Thus, electrical migration flux, being the most significant component in the transport of GAG chain and the aggrecan monomer in the articular cartilage, is large enough to counter both diffusive and convective fluxes and to dominate the directions of net solute flux.

1.4 Objectives

The objective of the thesis is to characterize the bulk transport of CS GAG disaccharide through articular cartilage by: (1) measuring partition coefficient of disaccharide between articular cartilage and external solution, (2) quantifying the steady-state, diffusive flux of disaccharide through articular cartilage, and (3) measuring the effect of an applied electric field on the disaccharide diffusive flux in articular cartilage.

An understanding of the factors which affect solute movement through the articular cartilage matrix will help in understanding the role of the in solute transport under physiological conditions. Measurements of transport rate of the solute will enable the identification of the rate of delivery of therapeutic agents into pathologic tissues. Characterization of bulk transport of the solute through the matrix would also enable better interpretation of cartilage pathology.

Chapter II

Theoretical Considerations

2.1 Mechanisms of Solute Transport through Articular Cartilage

Solute transport through the articular cartilage consists of three mechanisms: diffusion, electrical migration and convection [3]. The Nernst-Planck solute flux equation is:

$$\Gamma_i = \phi\left(-\overline{D}_i \frac{\partial \bar{c}_i(x,t)}{\partial x} + \frac{z_i}{|z_i|}\mu_i \bar{c}_i E \right) + \bar{c}_i U$$

where Γ_i is the flux of solute i (moles/cm^2 sec), ϕ is the tissue porosity, $\overline{D}_i$ is the diffusion coefficient of solute i in articular cartilage (cm^2/sec), $\bar{c}_i$ is the intratissue concentration of solute i (moles/cm^3), z_i is the valence of solute i, μ_i is the mobility of solute i (cm^2/volt sec), E is the electric field (volt/cm), and U is the intratissue fluid velocity (cm/sec) with the Einstein ionic diffusivity and mobility relationship:

$$\frac{\overline{D}_i}{\mu_i} = \frac{RT}{|z_i|F}$$

where the Faraday constant F is 96,500 coulombs/mole, incorporate all three transport mechanisms to represent the one dimensional molar solute flux of a given ionic species moving through the articular cartilage. The ionic mobility and diffusivity relationship is a function of temperature alone. At room temperature of 25^{0}C, $\overline{D}_i/\mu_i$ equals to 25.7/|z| mV [3].

The articular cartilage matrix, containing fixed negatively charged groups, creates a Donnan potential across the interface when the tissue is in an electrolyte solution. The Donnan equilibrium partition relationship gives boundary conditions for the Nernst-Planck equation to model the mobile ionic solute transport and concentration within the articular cartilage. The intratissue ionic concentrations are related to the external concentrations by the Donnan equilibrium partition:

$$\left(\frac{\bar{c}_x}{c_x}\right)^{1/|z_x|} = \left(\frac{c_y}{\bar{c}_y}\right)^{1/|z_y|} = constant$$

where the x refers to cations and the y refers to anions. Combining ionic concentrations with the concentration of tissue's fixed charge groups, electroneutrality of the tissue is satisfied when:

$$\bar{\rho}_m / F + \sum z_i \bar{c}_i = 0$$

where $\bar{\rho}_m$ is the fixed charge density of tissue.

2.2 Electroosmosis in Articular Cartilage

The presence of the negative fixed charge density in articular cartilage gives rise to the electromechanical transduction behavior of the tissue. The flux of mobile ions is related to the current density, J, by:

$$J = \sum J_i = F \sum z_i \Gamma_i$$

where F is the Faraday constant. The electromechanics of transduction properties of the tissue are modeled using macroscopic non-equilibrium thermodynamic relations of DeGroot and Mazur:

$$\begin{bmatrix} \dot{U} \\ \dot{\gamma} \end{bmatrix} = \begin{bmatrix} -k_{11} & k_{12} \\ k_{21} & -k_{22} \end{bmatrix} \begin{bmatrix} \nabla P \\ \nabla V \end{bmatrix}$$

where P is the fluid pressure, V is the electric potential, k_{11} is the short circuit Darcy hydraulic permeability, k_{22} is the electrical conductivity, and k_{12} and k_{21} are the coupling coefficients. k_{12} and k_{21} are equal and defined as negative for tissues with negative fixed charge density [3].

Electroosmotic flow occurs in the articular cartilage when an electric field is imposed across the tissue. A Schematic of electroosmotic flow induced in the articular cartilage by an applied electric field is shown in Figure 2.1. Positive counterions predominate within the Debye length of the membrane containing immobilized negative charge distribution. The application of an electric field across the membrane causes migration of the mobile ions due to electrophoretic forces. The imbalance between the migration of cations towards the cathode and the anions towards the anode results in a net momentum transfer to the solvent, and thus induces convective fluid flow in the tis-

sue in the direction of the applied electric field. The direction and magnitude of the induced fluid flow depend on the value of the applied field, the fixed charge density of the tissue and the size, charge, and concentration of the transporting solute.

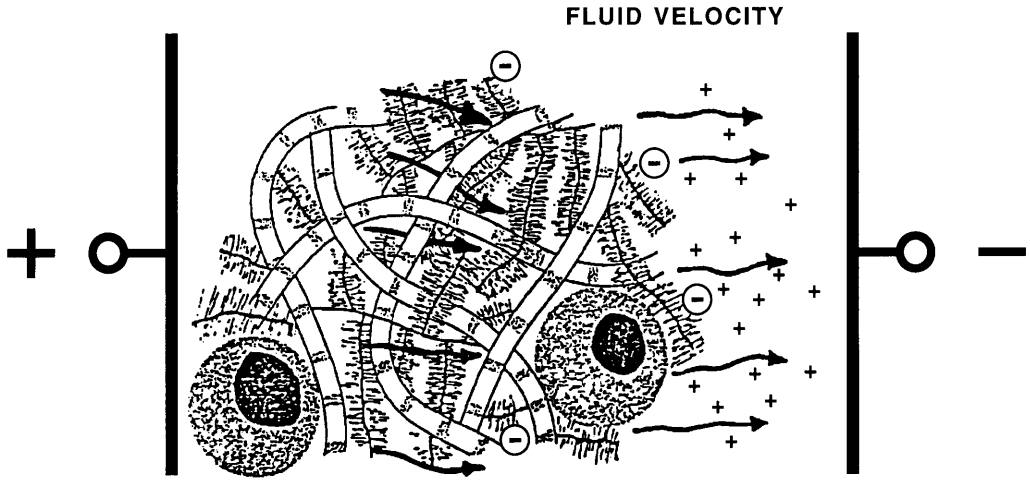

Figure 2.1: Schematic of electroosmotic flow induced in the articular cartilage by an electric field adapted from [2].

Chapter III

Methods

3.1 Articular Cartilage Dissection

Articular cartilage tissues used in experiments were harvested from the femoropatellar groove of adult steers purchased from Bertolino Beef, Boston, MA. Cylindrical cores 9mm in diameter were drilled out from the joints. The cores were individually clamped on a sledge microtome and positioned so that the top surface of the core was parallel to the microtome blade. Slices of superficial cartilage were removed from each core to obtain a flat top cartilage surface. Plane parallel disks of 200μm or 400μm thickness were then obtained and punched to 3mm or 9mm in diameter. Throughout the dissection process, tissues were maintained cold over ice and hydrated with 0.15M phosphate buffered saline (PBS) supplemented with 2mM EDTA plus 1ml/100ml dilution of penicillin (100 U/ml), streptomycin (0.1 mg/ml) and amphotericin B (0.25 μg/ml). All tissues were maintained in the phosphate buffered saline solution at 4°C overnight.

3.2 Disaccharide Preparation

^{35}S-sulfate labelled chondroitin sulfate disaccharides were generously provided by Doctor Anna Plaas. Four 100mm plates of rat chondrosarcoma cells were radiolabelled with 50 μCi/ml ^{35}S-sulfate in 10ml of DMEM/10% FCS for 24 hours. The medium was removed, and the cell layers were digested with 10μl of papain in 5ml of 50mM sodium acetate, pH 5.5, at 37°C for 18 hours. GAGs were precipitated with 95% ethanol and the precipitates dried. Pellets were dissolved in 500μl of 500mM ammonium acetate, pH 7.0, and chromatographed on Superose 6. Figure 3.1 shows the Superose 6 chromatography. Fractions 16 to 26 were pooled, lyophilized, washed with water and relyophilized. Relyophilized solutes were dissolved in 800μl of 0.1M sodium acetate, pH 7.4, digested with 500 mUnits of chondroitinase ABC at 37°C for 4 hours, and spun through a Microcon 3 filtration step. The specific activity of the product was measured as 5.5 X 10^6 CPM per 6.0mg of disaccharide. The product was then neutralized on ice with glacial acetic acid, speed-vaced, and washed two times with 500μl of ice cold methanol. The reduced solute was chromatographed on ToyoPeral HW40S in 500mM ammonium acetate at pH 7.0. Figure 3.2 shows the ToyoPearl HW40S chromatography. Fractions 45 to 51 were pooled, frozen, lyophilized, washed

with water, and relyophilized. The radioactivity associated with the final disaccharide content was reported as 300 X 10^6 CPM.

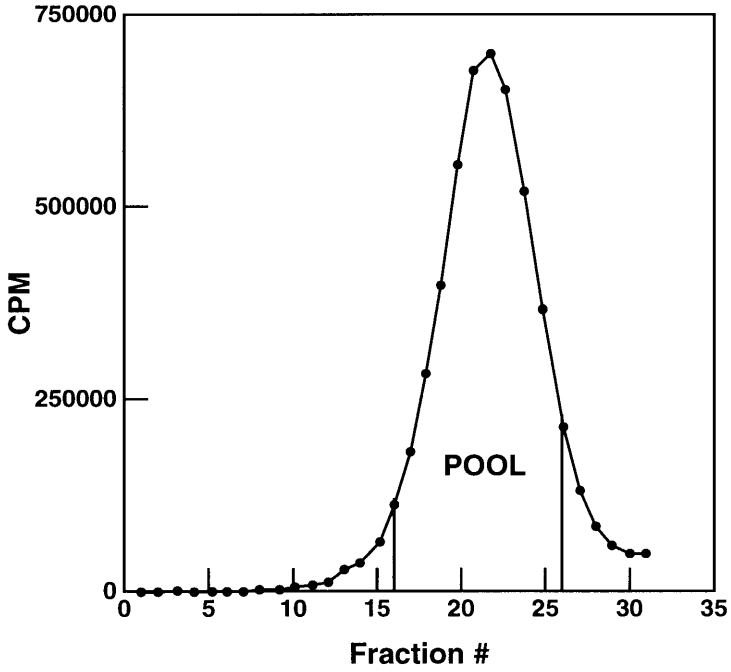

Figure 3.1: Superose 6 chromatography.

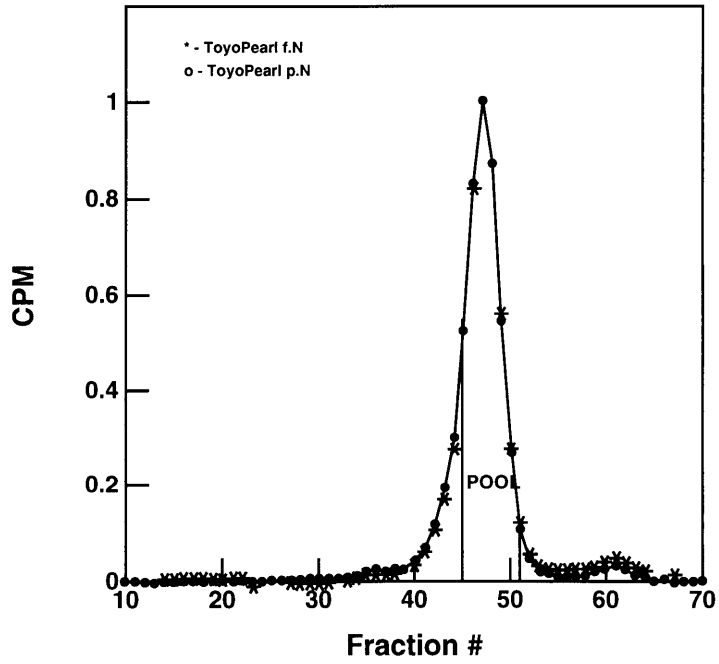

Figure 3.2: ToyoPearl HW40S chromatography.

3.3 Chondroitin Sulfate Preparation

Chondroitin sulfate C from Sigma was processed to remove salts and low molecular weight fragments. The chondroitin sulfate were papain digested overnight. The digested solute was boiled for 15 minutes, and then centrifuged at 5000G for half a hour. Supernatants were transferred into a vial, dissolved with 2 volumes of 0.1M sodium acetate in 100% ethanol, and spun at 5000G for 15 minutes. Supernatants were then removed and discarded. Pellets were lyophilized overnight, and finally dissolved in 0.15M PBS with 2mM EDTA. The final concentration of chondroitin sulfate was 20 mg/ml.

3.4 Salt Bridge Preparation

Salt bridges were made of cross-linked polyacrylamide (PA) using electrophoresis grade acrylaminde and N,N'-methylene-bis-acrylaminde crosslinker. The crosslinker content was 2.7% of the total monomer and the total monomer concentration was 10% in solution. One salt bridge consists of: 0.5g of 37.5:1 acrylaminde/N,N'-methylene-bis-acrylaminde crosslinker from Bio-Rad dissolved in 5ml of water, plus 3.3ul of 40% ammonium persulfate and 3.3ul of TEMED as initiators. The salt bridge was cast in a plexiglass tube with two layers of dialysis membrane secured to the bottom end with Teflon tape. A thin layer of water was gently applied over the surface with a Pasteur pipet to prevent oxygen from inhibiting the polymerization initiators. The salt bridge was left to polymerize at room temperature for 3 hours, and then it was stored in 1.5M of sodium chloride at $4^{o}C$.

3.5 Disaccharide Partition Measurements

Articular cartilage disks with thickness of 200μm or 400μm and diameter of 3mm or 9mm were obtained. Wet weight and thickness measurements were taken for every tissue disk. The tissues were then divided into various conditions, and equilibrated in PBS solutions containing ^{35}S-sulfate labelled disaccharides supplemented with proteinase inhibitors and 20 mg/ml of chondroitin sulfate. The proteinase inhibitor cocktail consisted of: 0.1mM of PMSF in isopropanol, 0.5mM of Benzamidine-HCl in ethanol, and 2mM of EDTA. Equilibration conditions varied with the temperature, the equilibration time and the desorption time. Table 3.1 lists five different disaccharide partition measurements conducted.

Tissue disks were removed from media after the equilibration and desorption period, washed briefly in PBS, patted dry, and measured for wet weights. Tissues were then lyophilized, weighed

dry and digested with papain solution, pH 6.0 at 60°C for 12 hours. The papain digestion solution consisted of: 125 μg/ml papain, 0.1M sodium phosphate, 5mM of Na_2-EDTA, and 5mM cysteine-HCl. Aliquots of the digests and equilibrating solutions were assessed for radioactivity by liquid scintillation counting. GAG assays were performed on the digests.

Measurement #	Diameter (mm)	Thickness (μm)	Temperature (°C)	Equilibration time	Desorption time	n
1	3	200	37	24 hours	0	4
				48 hours		4
2	9	200	37	24 hours	0	4
				48 hours		4
3	9	400	37	48 hours	0	4
			20			4
4	3	400	20	72 hours	0	5
				96 hours		5
5	9	400	20	24 hours	24 hours	5
				48 hours	48 hours	5

Table 3.1: Disaccharide partition measurements.

3.6 Disaccharide Transport Measurements

The transport apparatus, shown in Figure 3.3, consisted of two compartments separated by a partition. The partition, with five circular apertures, mounted up to five cartilage disks of 9mm in diameter. Tissue area exposed to solute transport after mounting was 0.38cm^2 per cartilage disk. Rubber gaskets and o-rings were used to mount various thickness of cartilage disks onto the partition, and to provide a tight seal between the two transport compartments. Transport between the upstream bath and the downstream bath was ensured to occur only through the cartilage tissue after the plexiglass transport apparatus were assembled.

Cooling coils and temperature probes were immersed in the bath of both compartments to maintain solutions at 20°C. The cooling coils were consisted of circulated refrigerated potassium dichromate solution in teflon tubes. A HAAKE A81 refrigerated circulator was used to maintain the potassium dichromate at a steady temperature of 20°C. The temperature probes were used to

monitor the temperature of the baths. Fluid in both baths was magnetically stirred to maintain homogeneity, and to minimize stagnant layer effects on transport. Platinum electrodes were used to apply current densities across the tissue disks mounted in the transport chamber. The electrodes were immersed in PBS solution supplemented with 25mM HEPES in contact with salt bridges. The salt bridges were immersed in the upstream and downstream bath during current applications. The downstream bath was continuously recirculated at approximately 1 ml/minute through a calcium-fluoride salt, solid scintillant cell in a Radiomatic Flo-One detector by Packard Instrument Company, Meriden, CT. The detector was used to monitor the radioactivity in the solid scintillant cell and to interface with a computer that sampled and recorded the radioactivity data every six seconds.

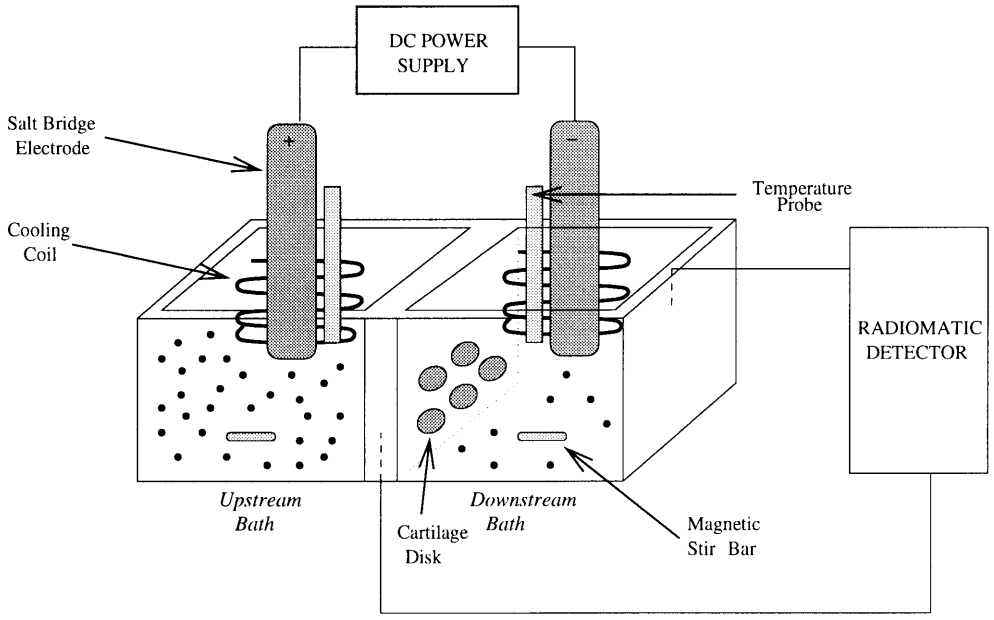

Figure 3.3: Schematic of the transport chamber adapted from [8].

Articular cartilage disks with thickness of 200μm or 400μm and diameter of 9mm were obtained. Wet weight and thickness measurements were taken individually for every tissue disk. The transport chamber was assembled with five tissue disks, and both chamber compartments were filled with 50ml of PBS solution supplemented with proteinase inhibitors and 20 mg/ml of chondroitin sulfate. The chamber was checked for leakage, and one hour of background radioactivity measurement of the downstream bath was made. The ^{35}S-sulfate labelled disaccharides were then added to the upstream bath, and the steady state diffusion was obtained. A radioactive disaccharide concentration calibration was performed by transferring a known aliquot volume $V_{u,cal}$

from the upstream bath into the downstream bath, and measuring the increase in downstream radioactivity $\Delta CPM_{d,\,cal}$. The upstream radiolabelled disaccharide concentration, $c_{di,u}$, was then calculated as:

$$c_{di,\,u} = \frac{\Delta CPM_{d,\,cal} V_d}{V_{u,\,cal}}$$

where V_d is the volume of downstream bath. Various current densities were applied across the articular cartilage. The pH of the solution in both compartments was monitored with litmus paper to be within pH 6-7 during current applications. Table 3.2 lists the five different disaccharide transport measurements conducted.

Measurement #	Thickness (μm)	$V_{u,cal}$ (μl)	n
1	200	500	5
2	200	500	5
3	200	500	5
4	200	500	5
5	400	1000	3

Table 3.2: Disaccharide transport measurements.

Current densities were applied across the articular cartilage in the five disaccharide transport measurements as follows:

1. Current densities in the sequence of -26 mA/cm^2, +26 mA/cm^2, and -26 mA/cm^2 were applied for 75 minutes at each level. The time between each current application was at least 65 minutes.
2. Current densities in the sequence of -26 mA/cm^2, +26 mA/cm^2, -26 mA/cm^2, and +26 mA/cm^2 were applied for 55 minutes at each level. The time between each current application was at least 25 minutes.
3. Current densities in the sequence of -26 mA/cm^2, -26 mA/cm^2, -26 mA/cm^2, +26 mA/cm^2, +26 mA/cm^2, and +26 mA/cm^2 were applied for 40 minutes at each level. The time between each current application was 40 minutes.

4. Current densities in the sequence of -16 mA/cm^2, +16 mA/cm^2, -26 mA/cm^2, +26 mA/cm^2, -36 mA/cm^2, +36 mA/cm^2, -16 mA/cm^2, +16 mA/cm^2, -26 mA/cm^2, +26 mA/cm^2, -36 mA/cm^2, and +36 mA/cm^2 were applied for 35 minutes at each level. The time between each current application was at least 50 minutes.
5. Current densities in the sequence of -16 mA/cm^2, +16 mA/cm^2, -26 mA/cm^2, +26 mA/cm^2, -36 mA/cm^2, and +36 mA/cm^2 were applied for 30 minutes at each level. The time between each current application was one hour.

Articular cartilage slices were removed from the transport chamber after the transport measurements, rinsed with PBS solution, lyophilized, weighed dry, and papain digested. Aliquots of the upstream and downstream baths were assessed for radioactivity by liquid scintillation counting. GAG assays were performed on the digests.

Chapter IV

Results

4.1 Disaccharide Partition Measurements

The disaccharide partition coefficient between the articular cartilage and the equilibrating medium, K_{di}, was calculated as:

$$K_{di} = \frac{CPM_t}{CPM_m}$$

where CPM_t is the total counts per minute of radiolabeled disaccharide in the tissue normalized to the water content of the tissue, and CPM_m is the total counts per minute of radiolabeled disaccharide in the equilibrating medium normalized to the medium volume. Table 4.1 lists the calculated disaccharide partition coefficients.

Measurement #		CPM_t (10^5)	CPM_m (10^5)	K_{di}	$K_{di} \pm SD$	$K_{di} \pm SD$
1	24 hours	11.5	21.62	0.53	37°C	1.12 ± 0.52
	48 hours	12.10	23.90	0.51	0.85 ± 0.51	
2	24 hours	17.02	23.12	0.74		
	48 hours	15.65	24.44	0.64		
3	37°C	6.96	3.77	1.85		
	20°C	7.23	3.76	1.92	20°C	
4	72 hours	2.24	2.30	0.97	1.38 ± 0.39	
	96 hours	1.89	2.07	0.91		
5	24 hours	1.19	0.72	1.65		
	48 hours	1.01	0.70	1.44		

Table 4.1: Calculated disaccharide partition coefficients between the articular cartilage and the equilibrating medium.

4.2 Disaccharide Transport Measurements

The steady state diffusion of disaccharide through the articular cartilage results in a linear increase of radioactivity, CPM_d, in the downstream compartment. The steady state disaccharide diffusive flux, Γ_{di}, was then calculated from the change in downstream concentration, ΔCPM_d, during a time interval, Δt, as:

$$\Gamma_{di} = \frac{\Delta CPM_d}{\Delta t}\frac{V_d}{A}$$

where V_d is the volume of downstream compartment, and A is the total cross-sectional tissue area exposed to disaccharide transport. Plots of the downstream radiolabelled disaccharide CPM versus time from the five transport measurements are shown in Appendix B. Figure 4.1, 4.2, 4.3, 4.4, and 4.5 show plots of the measured disaccharide flux in the articular cartilage normalized to the steady state diffusive flux in the presence of current application versus applied current density for disaccharide transport measurements #1, #2, #3, #4, and #5 respectively. The disaccharide diffusion coefficient in the articular cartilage, $\overline{D}_{di}$, was calculated by equating the measured disaccharide steady state diffusive flux, Γ_{di}, to the first term of the Nernst-Planck solute flux equation:

$$\Gamma_{di} = \overline{D_{di}}\frac{\partial \overline{c_{di}}(x,t)}{\partial x}$$

with

$$\frac{\partial \overline{c_{di}}(x,t)}{\partial x} = \frac{K_{di}c_u}{\delta} = \frac{K_{di}\Delta CPM_{d,cal}V_d}{\delta V_{u,cal}}$$

where δ is the tissue thickness, and K_{di} is the calculated disaccharide partition coefficient. The disaccharide diffusion coefficient in the articular cartilage, $\overline{D}_{di}$, was then calculated as:

$$\overline{D_{di}} = \frac{1}{K_{di}}\frac{\delta V_{u,cal}}{A\Delta CPM_{d,cal}}\left(\frac{\Delta CPM_d}{\Delta t}\right)$$

Table 4.2 lists the calculated disaccharide diffusion coefficients for each measurements. Hydration and GAG content values of the articular cartilage disks are listed in Appendix B.

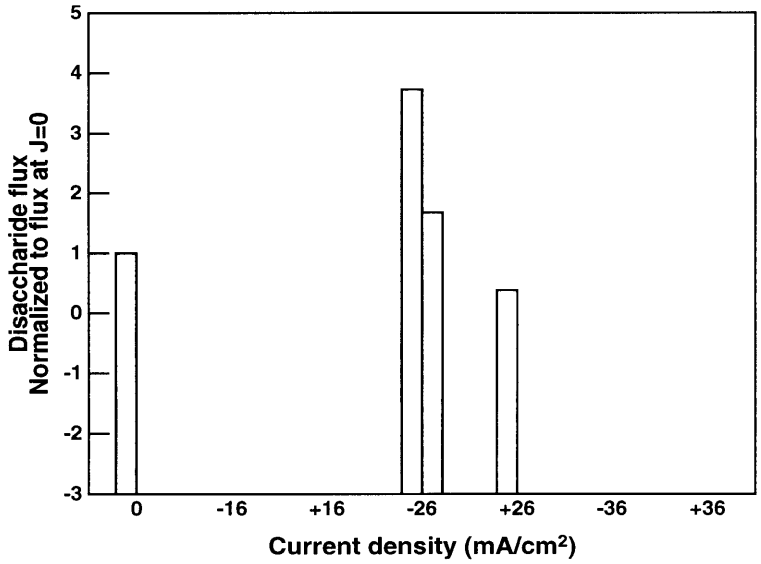

Figure 4.1: Plots of the measured disaccharide flux in the articular cartilage normalized to the steady state diffusive flux versus applied current density for disaccharide transport measurements #1.

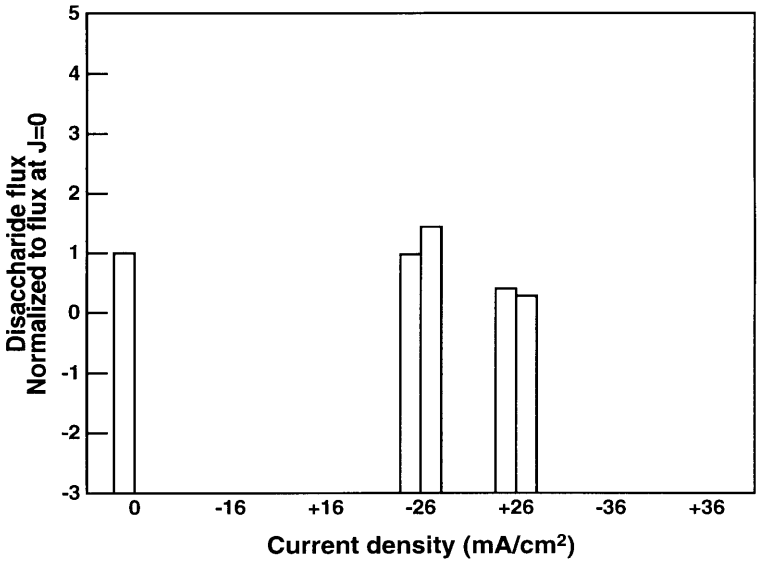

Figure 4.2: Plots of the measured disaccharide flux in the articular cartilage normalized to the steady state diffusive flux versus applied current density for disaccharide transport measurements #2.

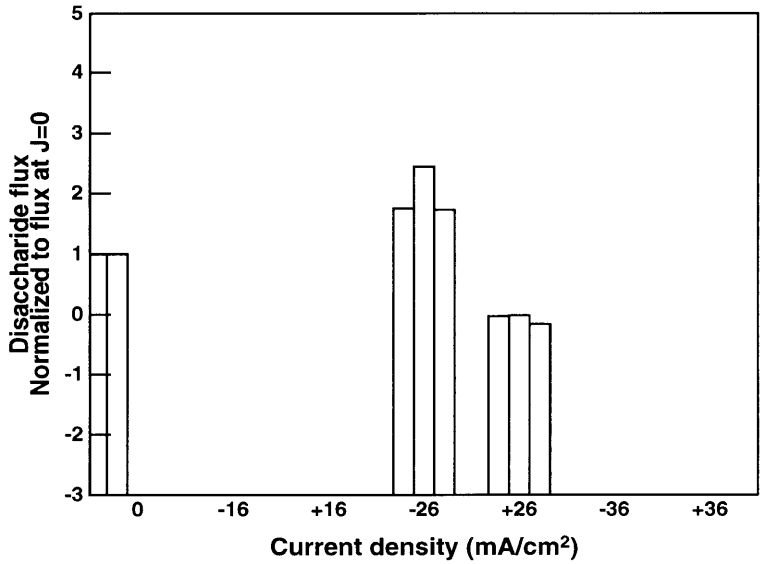

Figure 4.3: Plots of the measured disaccharide flux in the articular cartilage normalized to the steady state diffusive flux versus applied current density for disaccharide transport measurements #3.

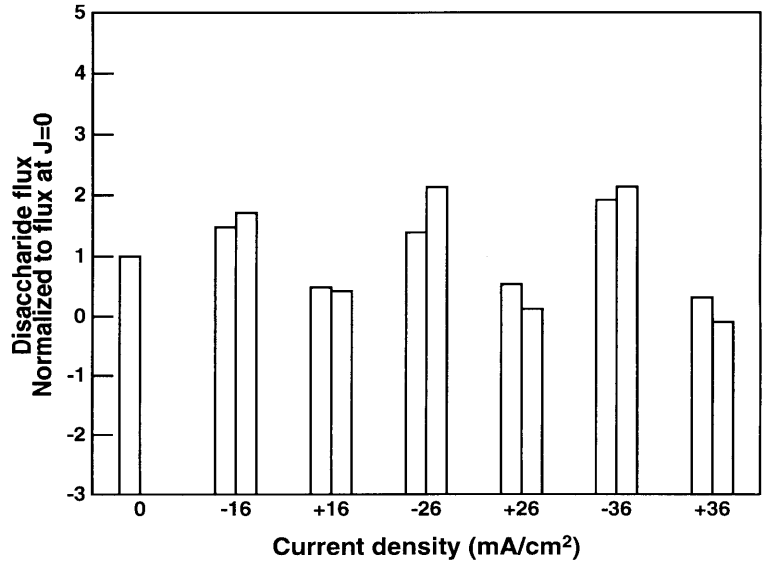

Figure 4.4: Plots of the measured disaccharide flux in the articular cartilage normalized to the steady state diffusive flux versus applied current density for disaccharide transport measurements #4.

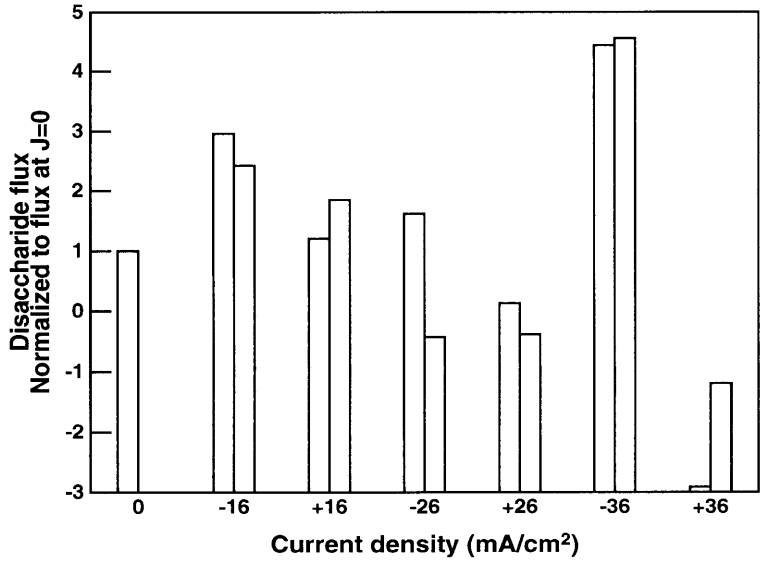

Figure 4.5: Plots of the measured disaccharide flux in the articular cartilage normalized to the steady state diffusive flux versus applied current density for disaccharide transport measurements #5.

Measurement #	$\Delta CPM_{d,cal}$	ΔCPM_d / Δt (CPM/sec)	$\overline{D}_{di}$ (10^{-6} cm^2/sec)	$\overline{D}_{di} \pm SD$ (10^{-6} cm^2/sec)
1	778.85	0.059	3.93	4.49 ± 1.13
2	604.92	0.058	4.98	
3	53.59	0.0033	3.21	
4	138.83	0.010	3.90	
5	69.87	0.0013	6.45	

Table 4.2: Calculated disaccharide diffusion coefficients in the articular cartilage.

Application of negative current densities across the articular cartilage elevated the disaccharide flux over the steady state diffusive flux by a factor of 2.36 ± 1.15 (mean$\pm$SD), and application of positive current densities depressed the disaccharide flux under the steady state diffusive flux by a factor of 0.055 ± 0.94 (mean$\pm$SD).

Chapter V

Discussion

5.1 Disaccharide Partition Measurements

In the five disaccharide partition measurements: no dependence was observed between the disaccharide partition coefficient and the tissue hydration, nor was the dependence observed between the disaccharide partition coefficient and the GAG content of the tissue. Hydration and GAG content values of the articular cartilage disks are listed in Appendix A. Plots of the calculated disaccharide partition coefficient versus tissue hydration and plots of the calculated disaccharide partition coefficient versus GAG content of the tissue are shown in Appendix A. The calculated disaccharide partition coefficient of 1.12 $\pm$ 0.52 (mean$\pm$SD) was higher than both the GAG chain partition coefficients and the aggrecan monomer partition coefficients calculated by Jen [8] between the articular cartilage and external solutions with fix charge densities of 20 mg/ml.

The disaccharide has a higher equilibrium uptake by the articular cartilage than the GAG chain and the aggrecan monomer, due to the smaller size of disaccharide. Due to the Donnan potential created across the negatively charged articular cartilage matrix and the also negatively charged disaccharide, one would predict a less than one partition coefficient for the disaccharide. The calculated disaccharide partition coefficient for partition measurements conducted under 37^{o}C was 0.85 $\pm$ 0.51 (mean$\pm$SD), less than one; however, the calculated disaccharide partition coefficient for partition measurements conducted under 20^{o}C was 1.38 $\pm$ 0.39 (mean$\pm$SD), greater than one.

5.2 Disaccharide Transport Measurements

The calculated disaccharide diffusion coefficients, 4.49 $\pm$ 1.13 X 10^{-6} cm^2/sec (mean$\pm$SD), in the articular cartilage was 10 times higher the GAG chain coefficients and 100 times higher than the aggrecan monomer coefficients calculated by Jen [8]. The effect of applied current densities on the disaccharide flux in the articular cartilage was not as significant as the effect of applied current densities on the GAG chain flux nor the aggrecan monomer flux measured by Jen [8]. The electrophoretic component of disaccharide flux during current application was not as significant as of the GAG chain flux and the aggrecan monomer flux in the articular cartilage to dominate the direction

of net flux, however, the electrical migration flux was still the most significant component in the transport of disaccharide.

The disaccharide has a larger diffusion coefficient and a smaller fluctuation in flux with applied current densities than the GAG chain and the aggrecan monomer in the articular cartilage, due to the smaller size of disaccharide.

5.3 Future Research

Disaccharide transport through the articular cartilage was studied by measuring the disaccharide partition coefficient and diffusion coefficient. The separation of the contributions to disaccharide transport of convection and electrophoretic migration from the effects of matrix consolidation as occurs during mechanical loading was studied by application of current density across the articular cartilage to induce an electroosmotic fluid flow.

The thesis has laid the ground work for several studies that can follow: studies involving superimposing graded levels of compression with the disaccharide transport measurement, studies involving disaccharide transport measurements under time-varying current application, and studies involving disaccharide transport through an intact articular cartilage surface.

Appendix A

Disaccharide Partition Measurements

The hydration and GAG content values of articular cartilage slices are calculated as:

$$Hydration = \frac{WetWeight - DryWeight}{DryWeight}$$

$$GAGContent = \frac{GAGWeight}{DryWeight} \times 100$$

Tables A.1, A.2, A.3, A.4, and A.5 list the hydration and the GAG content values of articular cartilage slices used in disaccharide partition measurements #1, #2, #3, #4, and #5, respectively, with the calculated disaccharide partition coefficients.

Time (hours)	Slice #	Hydration	GAG content	K_{di}
24	1	3.59	15.59	0.57
	2	2.49	11.90	0.60
	3	2.74	8.65	0.55
	4	2.08	12.66	0.41
mean±SD		2.73 ± 0.55	12.20 ± 2.47	0.53 ± 0.07
48	1	3.42	10.01	0.72
	2	3.41	13.23	0.30
	3	2.48	11.86	0.60
	4	4.33	14.37	0.41
mean±SD		3.41 ± 0.65	12.36 ± 1.63	0.51 ± 0.16

Table A.1: Hydration and GAG content values of articular cartilage disks used in disaccharide partition measurement #1. 3mm diameter, 200μm thick articular cartilage disks were equilibrated at 37°C.

Time (hours)	Slice #	Hydration	GAG content	K_{di}
24	1	4.47	8.77	0.70
	2	4.68	6.89	0.38
	3	2.37	9.64	0.36
	4	3.28	10.24	1.50
mean±SD		3.70 ± 0.94	8.89 ± 1.26	0.74 ± 0.46
48	1	2.72	12.37	0.34
	2	2.49	10.36	0.36
	3	2.91	17.58	0.25
	4	2.58	11.96	1.63
mean±SD		2.68 ± 0.16	13.07 ± 2.71	0.65 ± 0.57

Table A.2: Hydration and GAG content values of articular cartilage disks used in disaccharide partition measurement #2. 9mm diameter, 200μm thick articular cartilage disks were equilibrated at 37°C.

Temperature	Slice #	Hydration	GAG content	K_{di}
37°C	1	5.20	4.53	1.77
	2	3.37	2.63	1.86
	3	3.88	2.89	1.81
	4	3.73	3.23	1.94
mean±SD		4.05 ± 0.69	3.32 ± 0.73	1.85 ± 0.06
20°C	1	3.39	2.87	2.56
	2	4.07	3.60	1.79
	3	3.73	3.16	1.85
	4	3.36	3.09	1.49
mean±SD		3.64 ± 0.29	3.18 ± 0.27	1.92 ± 0.39

Table A.3: Hydration and GAG content values of articular cartilage disks used in disaccharide partition measurement #3. 9mm diameter, 400μm thick articular cartilage disks were equilibrated for 48 hours.

Time (hours)	Slice #	Hydration	GAG content	K_{di}
72	1	5.74	15.74	1.00
	2	5.58	15.17	1.16
	3	7.05	16.57	0.92
	4	3.53	8.29	0.82
	5	4.17	9.33	0.96
mean±SD		5.21 ± 1.24	13.02 ± 3.48	0.97 ± 0.11
96	1	3.71	11.42	1.07
	2	6.13	21.22	0.85
	3	3.44	11.33	0.84
	4	3.03	11.90	0.92
	5	4.37	15.60	0.89
mean±SD		4.14 ± 1.09	14.29 ± 3.81	0.91 ± 0.08

Table A.4: Hydration and GAG content values of articular cartilage disks used in disaccharide partition measurement #4. 3mm diameter, 400μm thick articular cartilage disks were equilibrated at 20°C.

Time (hours)	Slice #	Hydration	GAG content	K_{di}
24	1	3.75	3.25	1.46
	2	3.17	3.02	1.72
	3	3.17	2.97	2.24
	4	4.99	2.41	1.45
	5	3.92	3.35	1.41
mean±SD		3.80 ± 0.67	3.00 ± 0.33	1.66 ± 0.31
48	1	2.56	3.04	3.48
	2	3.76	2.90	0.59
	3	3.28	3.71	0.66
	4	4.40	3.06	0.92
	5	3.20	3.10	1.54
mean±SD		3.44 ± 0.61	3.16 ± 0.28	1.44 ± 1.07

Table A.5: Hydration and GAG content values of articular cartilage disks used in disaccharide partition measurement #5. 9mm diameter, 400μm thick articular cartilage disks were equilibrated and desorbed at 20°C.

Figure A.1, A.2, A.3, A.4, and A.5 show plots of the calculated disaccharide partition coefficient versus tissue hydration and plots of the calculated disaccharide partition coefficient versus GAG content of the tissue for disaccharide partition measurements #1, #2, #3, #4, and #5 respectively.

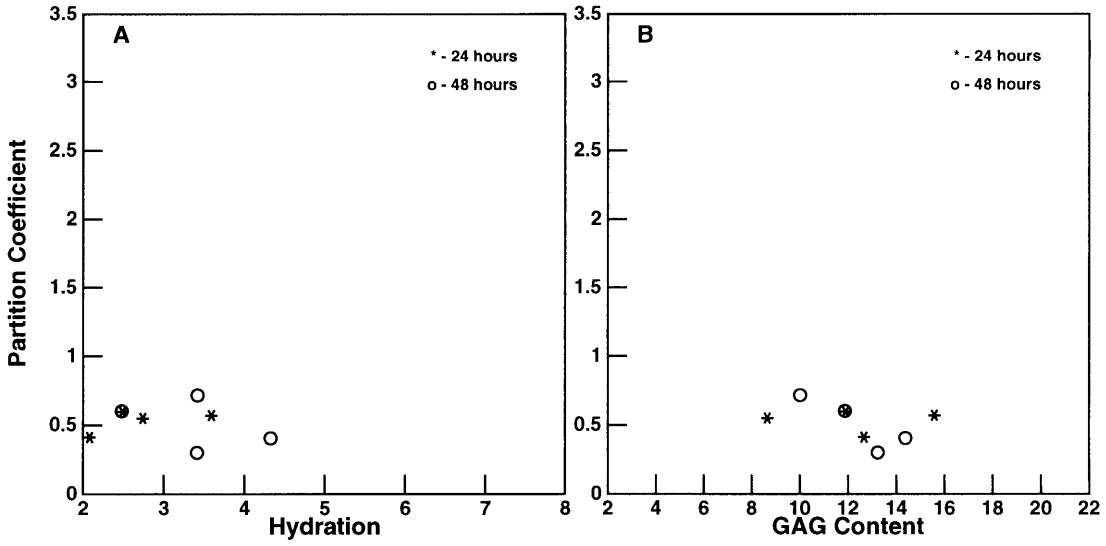

Figure A.1: Plots of the calculated disaccharide partition coefficient versus tissue hydration and GAG content of the tissue. A) Plot of the calculated disaccharide partition coefficient versus tissue hydration for disaccharide partition measurement #1. B) Plot of the calculated disaccharide partition coefficient versus GAG content of the tissue for disaccharide partition measurement #1.

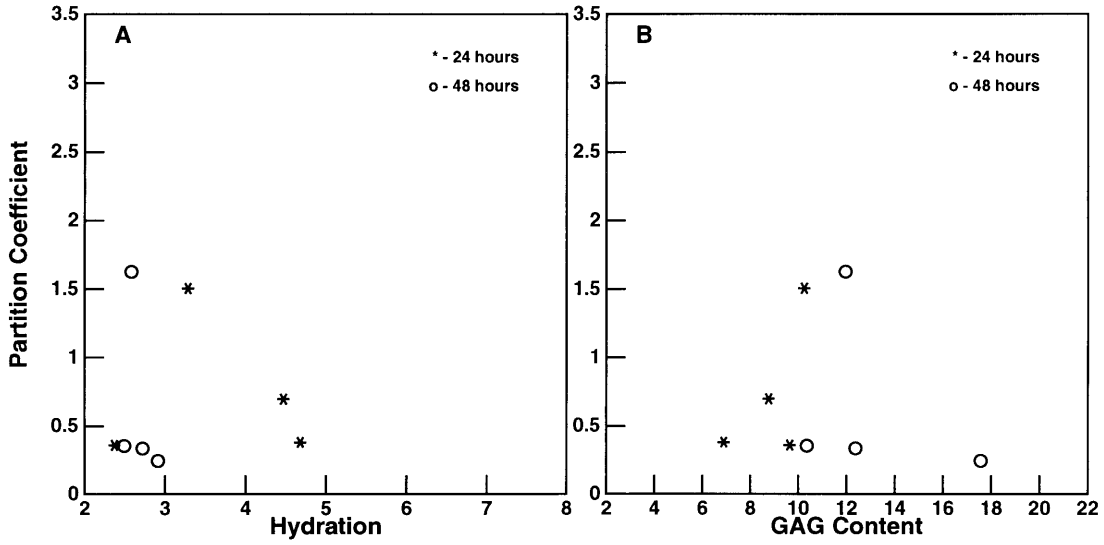

Figure A.2: Plots of the calculated disaccharide partition coefficient versus tissue hydration and GAG content of the tissue. A) Plot of the calculated disaccharide partition coefficient versus tissue hydration for disaccharide partition measurement #2. B) Plot of the calculated disaccharide partition coefficient versus GAG content of the tissue for disaccharide partition measurement #2.

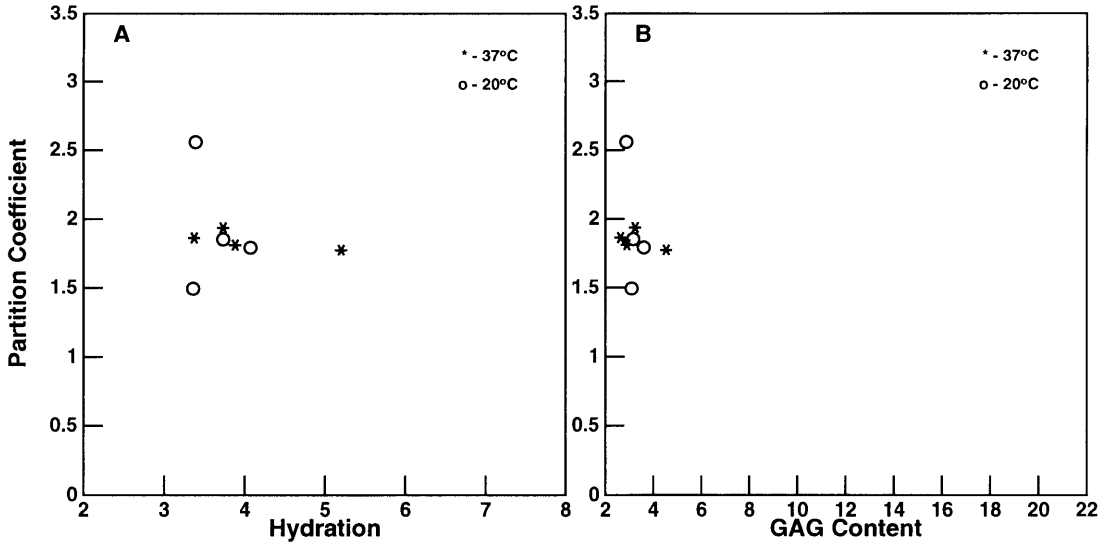

Figure A.3: Plots of the calculated disaccharide partition coefficient versus tissue hydration and GAG content of the tissue. A) Plot of the calculated disaccharide partition coefficient versus tissue hydration for disaccharide partition measurement #3. B) Plot of the calculated disaccharide partition coefficient versus GAG content of the tissue for disaccharide partition measurement #3.

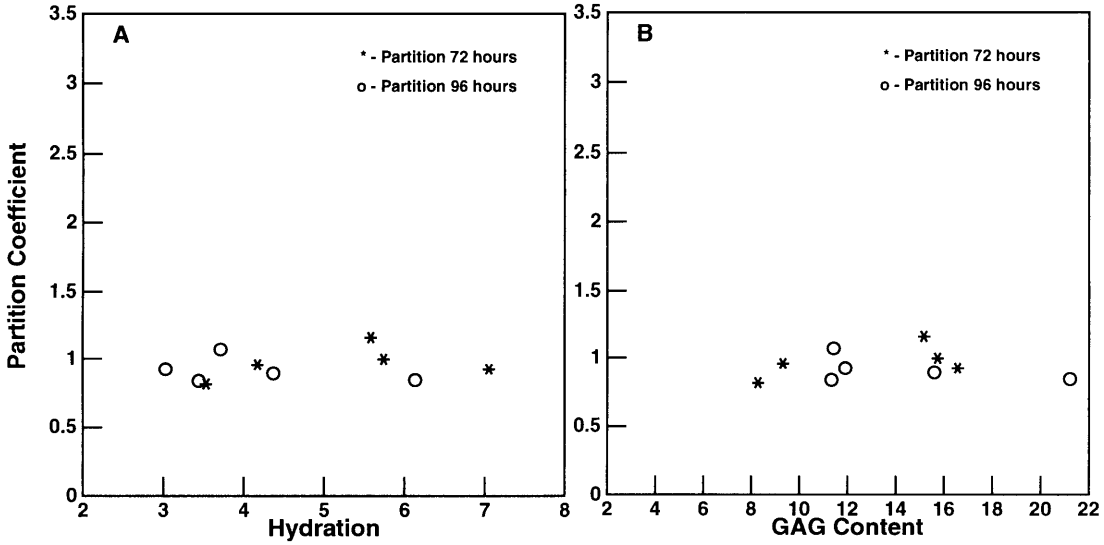

Figure A.4: Plots of the calculated disaccharide partition coefficient versus tissue hydration and GAG content of the tissue. A) Plot of the calculated disaccharide partition coefficient versus tissue hydration for disaccharide partition measurement #4. B) Plot of the calculated disaccharide partition coefficient versus GAG content of the tissue for disaccharide partition measurement #4.

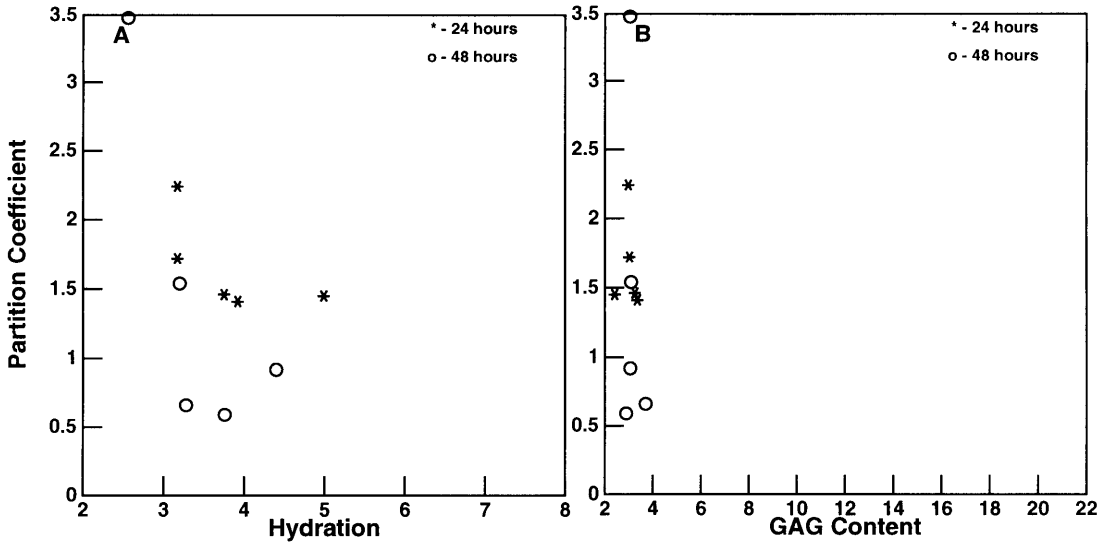

Figure A.5: Plots of the calculated disaccharide partition coefficient versus tissue hydration and GAG content of the tissue. A) Plot of the calculated disaccharide partition coefficient versus tissue hydration for disaccharide partition measurement #5. B) Plot of the calculated disaccharide partition coefficient versus GAG content of the tissue for disaccharide partition measurement #5.

Appendix B

Disaccharide Transport Measurements

The hydration and GAG content values of articular cartilage slices are calculated as:

$$Hydration = \frac{WetWeight - DryWeight}{DryWeight}$$

$$GAGContent = \frac{GAGWeight}{DryWeight} \times 100$$

Tables B.1, B.2, B.3, B.4, and B.5 list the hydration and the GAG content values of articular cartilage slices used in disaccharide transport measurements #1, #2, #3, #4, and #5, respectively, with the calculated disaccharide diffusion coefficients.

Slice #	Hydration	GAG content	$\overline{D}_{di}$ (cm^2/sec)
1	3.56	6.88	3.93×10^{-6}
2	5.28	10.39	
3	3.36	8.63	
4	4.01	5.09	
5	3.72	7.66	
mean±SD	3.99 ± 0.68	7.73 ± 1.77	

Table B.1: Hydration and GAG content values of 200μm thick articular cartilage disks used in disaccharide transport measurement #1.

Slice #	Hydration	GAG content	$\overline{D}_{di}$ (cm^2/sec)
1	3.02	8.85	4.98×10^{-6}
2	2.69	10.07	
3	3.74	12.03	
4	2.85	9.03	
5	3.57	10.07	
mean±SD	3.17 ± 0.41	10.01 ± 1.13	

Table B.2: Hydration and GAG content values of 200μm thick articular cartilage disks used in disaccharide transport measurement #2.

Slice #	Hydration	GAG content	$\overline{D}_{di}$ (cm^2/sec)
1	3.67	9.27	3.21×10^{-6}
2	2.78	9.58	
3	2.41	7.35	
4	3.16	7.22	
5	3.68	10.78	
mean±SD	3.14 ± 0.50	8.84 ± 1.37	

Table B.3: Hydration and GAG content values of 200μm thick articular cartilage disks used in disaccharide transport measurement #3.

Slice #	Hydration	GAG content	$\overline{D}_{di}$ (cm^2/sec)
1	4.34	11.74	3.90×10^{-6}
2	4.49	11.27	
3	3.45	13.69	
4	4.87	12.40	
5	3.03	9.29	
mean±SD	4.04 ± 0.69	11.68 ± 1.45	

Table B.4: Hydration and GAG content values of 200μm thick articular cartilage disks used in disaccharide transport measurement #4.

Slice #	Hydration	GAG content	$\overline{D}_{di}$ (cm^2/sec)
1	4.95	6.93	6.45×10^{-6}
2	4.59	7.68	
3	4.99	7.19	
mean±SD	4.84 ± 0.18	7.27 ± 0.31	

Table B.5: Hydration and GAG content values of 400μm thick articular cartilage disks used in disaccharide transport measurement #5.

Figures B.1, B.2, B.3, B.4, and B.5 show plots of the disaccharide radioactivity CPM of the downstream bath versus time for transport measurements #1, #2, #3, #4, and #5 respectively.

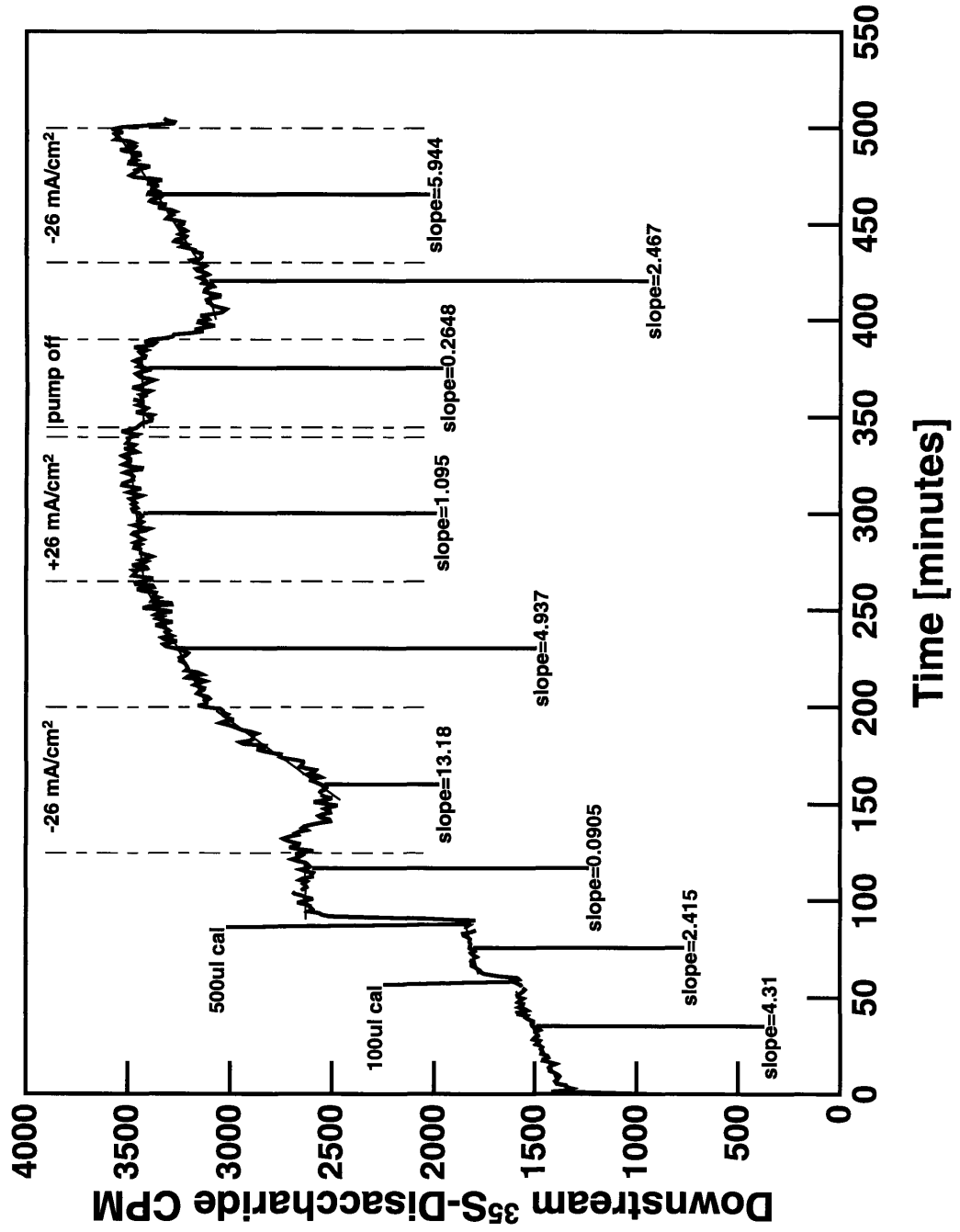

Figure B.1: Plot of the downstream radiolabelled disaccharide CPM versus time from transport measurement #1.

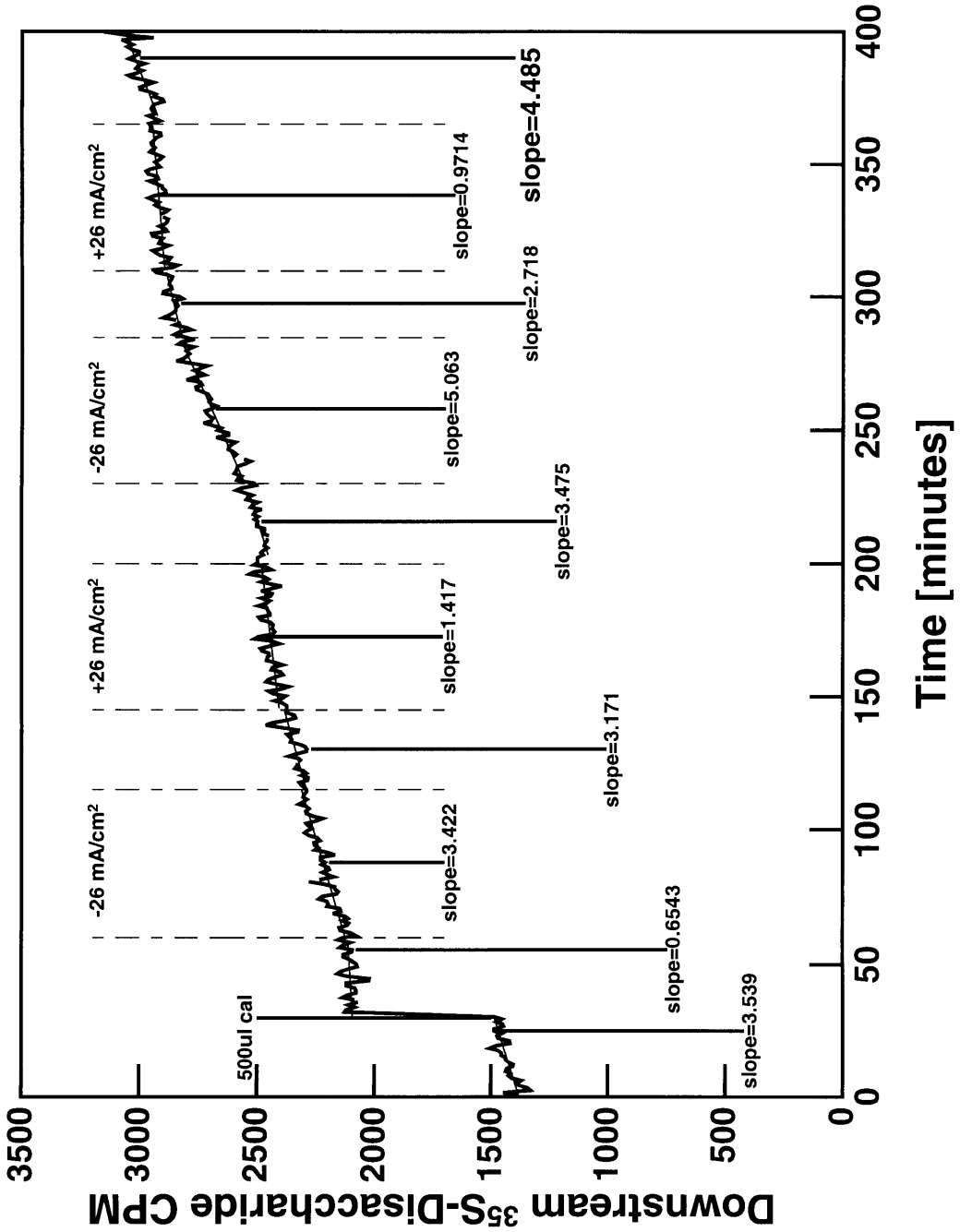

Figure B.2: Plot of the downstream radiolabelled disaccharide CPM versus time from transport measurement #2.

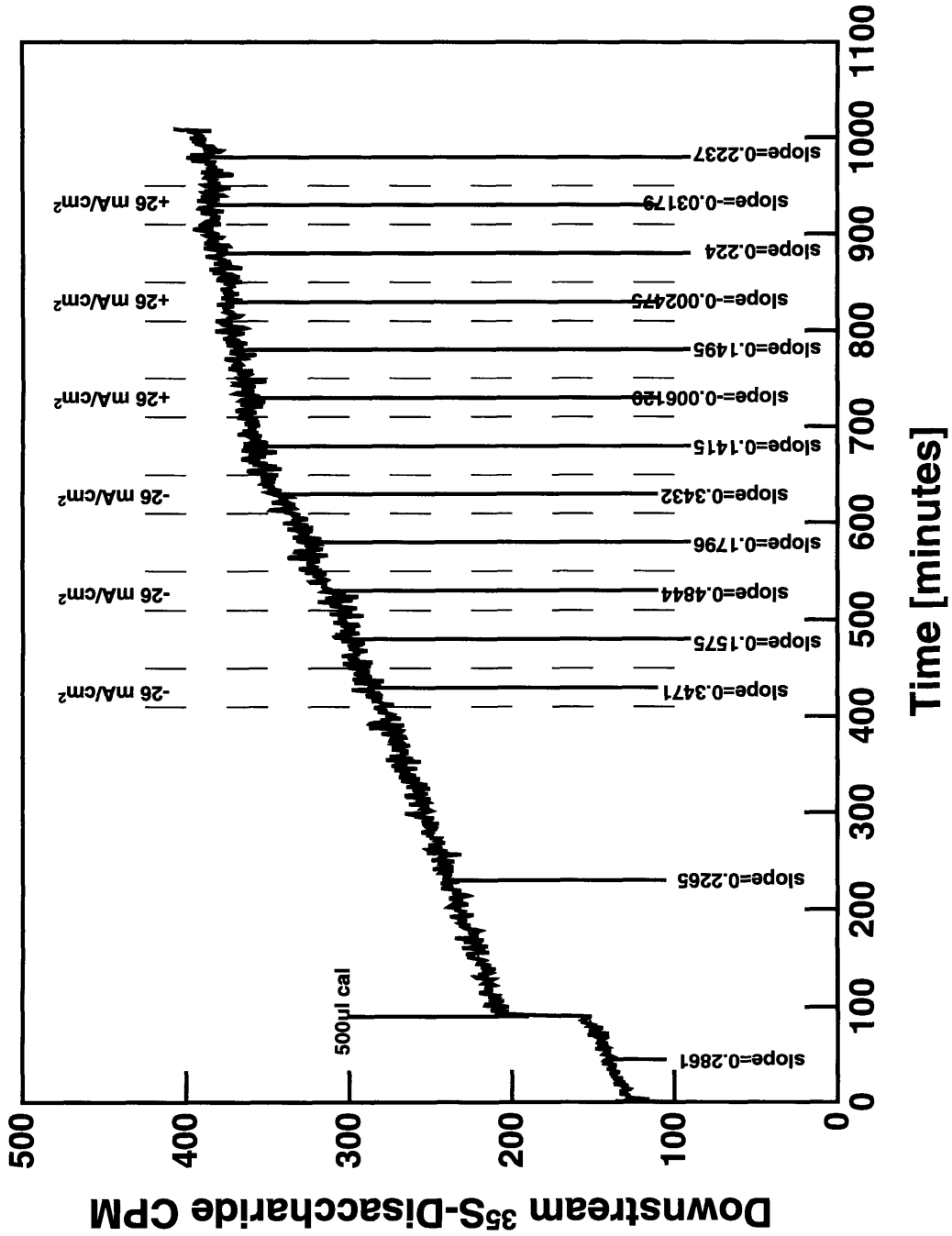

Figure B.3: Plot of the downstream radiolabelled disaccharide CPM versus time from transport measurement #3.

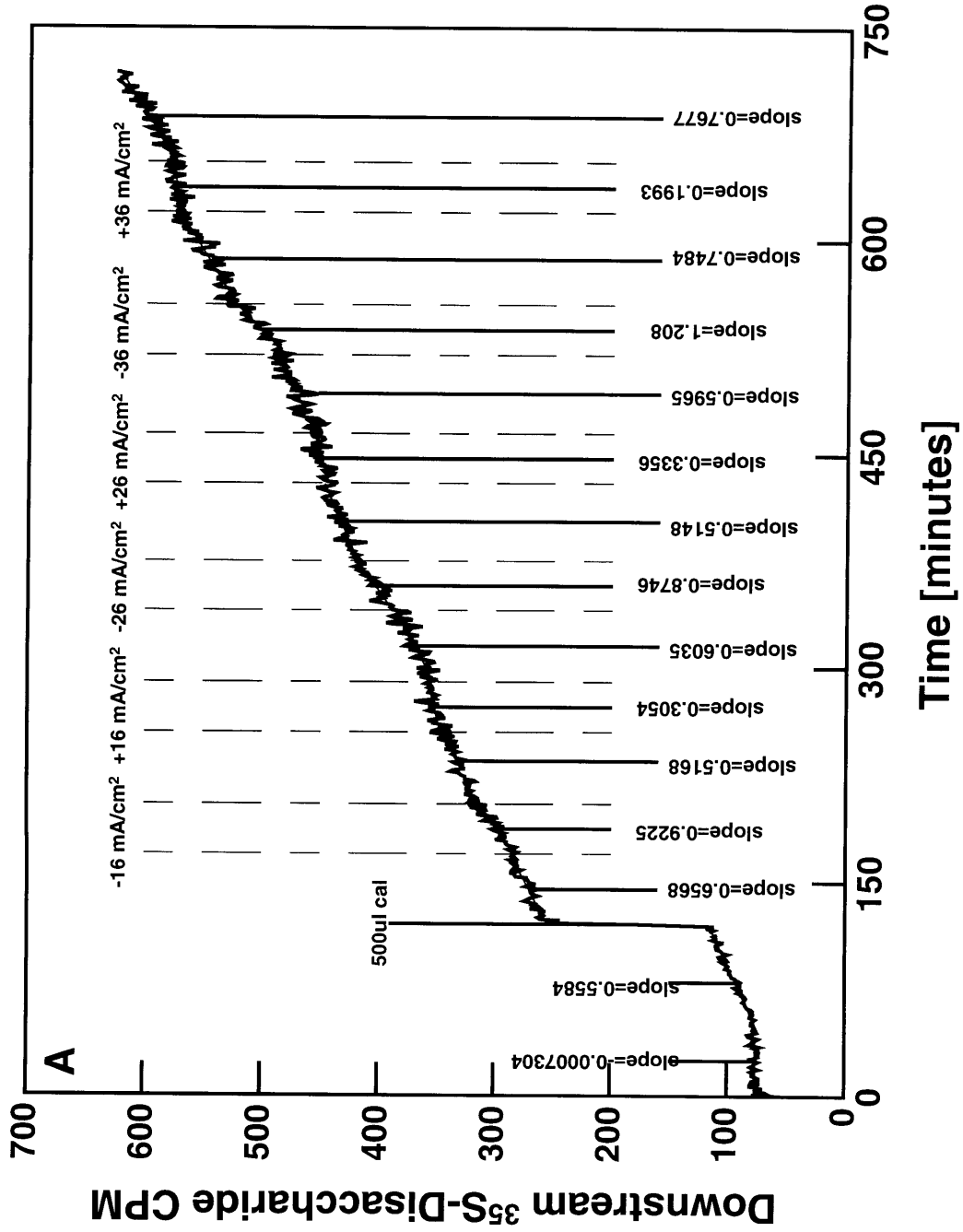
A
Downstream 35S-Disaccharide CPM
Time [minutes]
0
150
300
450
600
750
100
200
300
400
500
600
700
slope=0.0007304
slope=0.5584
500ul cal
slope=0.6568
slope=0.9225
slope=0.5168
slope=0.3054
slope=0.6035
slope=0.8746
slope=0.5148
slope=0.3356
slope=0.5965
slope=1.208
slope=0.7484
slope=0.1993
slope=0.7677
-16 mA/cm2 +16 mA/cm2 -26 mA/cm2 +26 mA/cm2 -36 mA/cm2 +36 mA/cm2

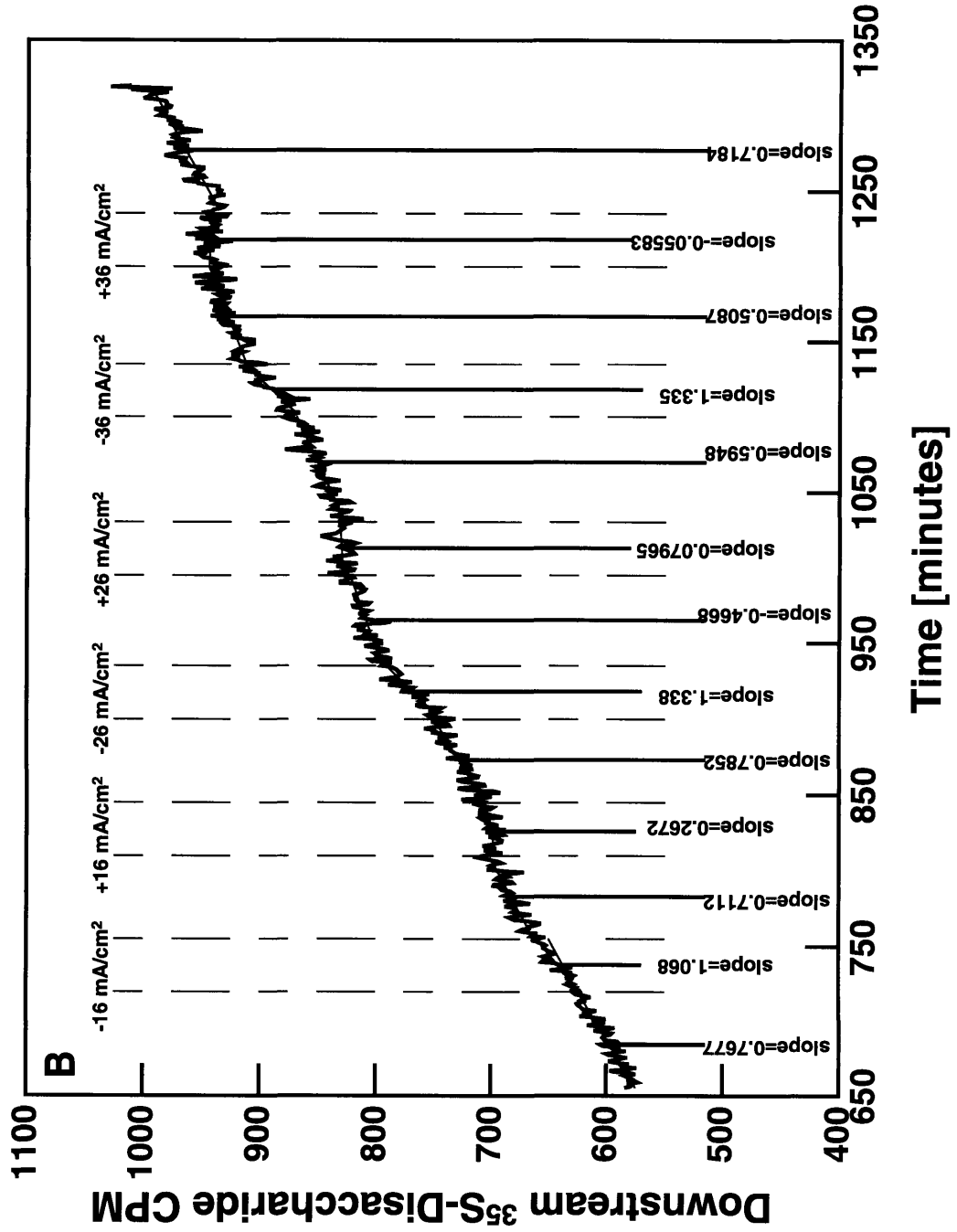

Figure B.4: Plots of the downstream radiolabelled disaccharide CPM versus time from transport measurement #4.

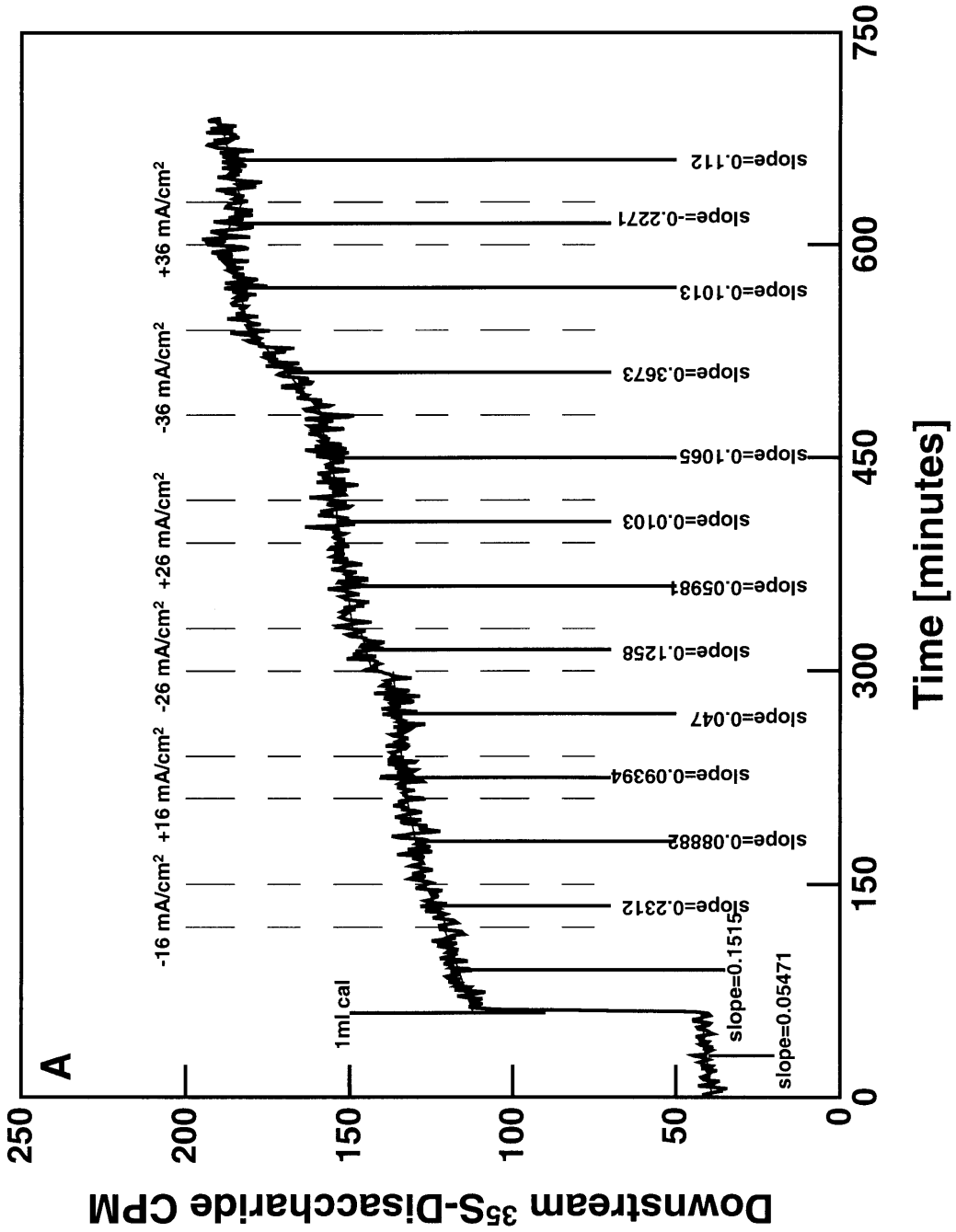
A
Downstream 35S-Disaccharide CPM
Time [minutes]
0
50
100
150
200
250
0
150
300
450
600
750
-16 mA/cm2
+16 mA/cm2
-26 mA/cm2
+26 mA/cm2
-36 mA/cm2
+36 mA/cm2
1ml cal
slope=0.05471
slope=0.1515
slope=0.2312
slope=0.08882
slope=0.09394
slope=0.047
slope=0.1258
slope=0.05981
slope=0.0103
slope=0.1065
slope=0.3673
slope=0.1013
slope=-0.2271
slope=0.112

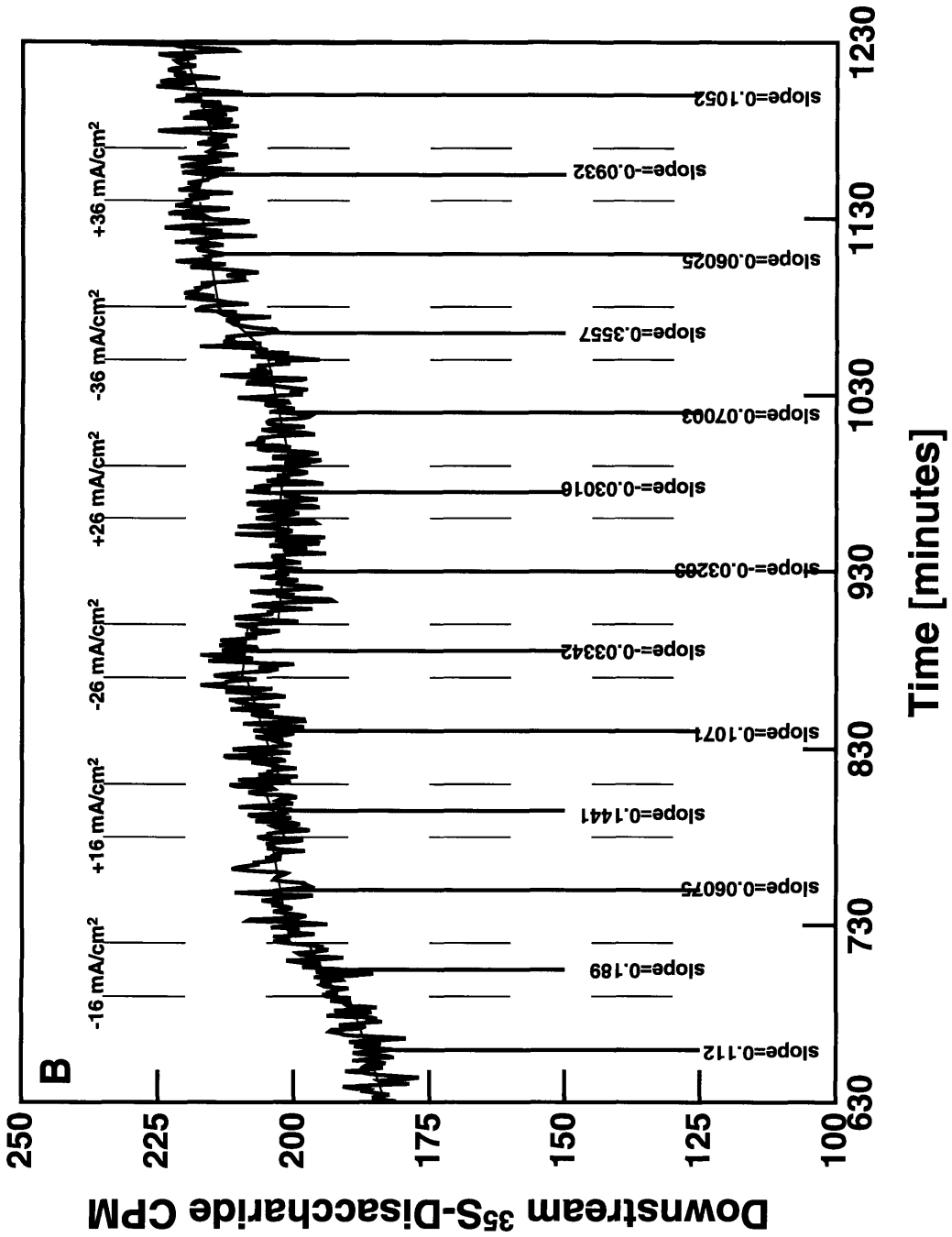

Figure B.5: Plots of the downstream radiolabelled disaccharide CPM versus time from transport measurement #5.

Bibliography

[1] Buckwalter J, Hunziker E, Rosenberg L, Coutts R, Adams M, Eyre D: Articular cartilage: composition and structure. In Woo SLY, Buckwalter JA, editors, *Injury and repair of the musculoskeletal soft tissues*, pages 405-425. American Academy of Orthopaedic Surgeons, ParkRidge, IL, 1988.

[2] Garcia AM: *Mechanisms of Macromolecular Transport Through Articular Cartilage: Relevance to Loading.* Doctor of Philosophy thesis, Massachusetts Institute of Technology, Cambridge, MA, 1996.

[3] Grodzinsky AJ: Electromechanical and physicochemical properties of connective tissue. *CRC Crit Rev Bioeng*, 9:133-199, 1983.

[4] Grodzinsky AJ: *Fields, Forces and Flows in Biological Tissues and Membranes.* Massachusetts Institute of Technology, Cambridge, MA, 1992.

[5] Gray ML, Pizzanelli AM, Grodzinsky AJ, Lee RC: Mechanical and physicochemical determinants of the chondrocyte biosynthetic response. *J Orthop Res*, 6:777-792, 1988.

[6] Gray ML, Pizzanelli AM, Lee RC, Grodzinsky AJ, Swann DA: Kinetics of the chondrocyte biosynthetic response to compressive load and release. *Biochim Biophys Acta*, 991:415-425, 1989.

[7] Heinegrad D, Oldberg A: Structure and biology of cartilage and bone matrix noncollageneous macromolecules. *FASEB*, 3:2042-2051, 1989.

[8] Jen MC: *Transport Studies of Component Proteoglycan Molecules through Cartilage.* Master of Engineering thesis, Massachusetts Institute of Technology, Cambridge, MA, 1995.

[9] Maroudas A: Distribution and diffusion of solutes in articular cartilage. *Biophys J*, 10:365-379, 1970.

[10] Maroudas A: Physicochemical properties of articular cartilage. In Freeman MAR, editor, *Adult Articular Cartilage, 2nd ed.*, pages 215-290. Pitman, Tunbridge Wells, England, 1979.

[11] Nimni ME, Harkness D: Molecular structures and functions of collagen. In Nimni ME, editor, *Collagen*, pages 1-77. CRC Press Inc., Boca Raton, 1988.

[12] Rosenberg L: Structure of cartilage proteoglycans. In PMC Burleigh, AR Poole, editors, *Dynamics of Connective Tissue Macromolecules*, pages 105-128. North-Holland Publishing Company, Amsterdam, 1975.

[13] Sah RL, Kim YJ, Doong JH, Grodzinsky AJ, Plaas AHK, Sandy JD: Biosythetic response of cartilage explants to dynamic compression. *J Orthop Res*, 7:619-636, 1989.

[14] Schneiderman R, Kevet D, Maroudas A: Effects of mechanical and osmotic pressure on the rate of glycosaminoglycan synthesis in the human adult femoral head cartilage: an in vitro study. *J Orthop Res*, 4:393-408, 1986.